Supporting Information

Perturbing Tumor Cell Metabolism with Ru(II) Photo-redox Catalyst to Reverse Multidrug Resistance of Lung Cancer

Siqi Wei[1+], Hui Liang[2+], Anyi Dao[1+], Yuzhen Xie[1], Fengshu Cao[3], Qingyan Ren[3], Ashish Kumar Yadav[4], Rajesh Kushwaha[4], Arif Ali Mandal[4], Samya Banerjee[4], Pingyu Zhang[3], Shaomin Ji[2*], Huaiyi Huang[1*]

Contents

Tables

References

Experimental section

Materials and measurements

Materials

All reagents and materials from commercial sources. $RuCl_3 \cdot 3H_2O$ and methylene blue trihydrate were purchased from Macklin. 2,2':6',2''-terpyridine was purchased from Sigma-Aldrich. 1-pyrenecarboxaldehyde, 2,6-diacetylpyridine, 2-aminonicotinaldehyde, cis-platin, ammonium hexafluorophosphate, chlorin e6 (Ce6), 2,2'-(anthracene-9,10-diylbis(methylene)) dimalonic acid (ABDA), Reactive Oxygen Species Assay Kit (ROS Assay Kit), β-Nicotinamide adenine dinucleotide disodium salt (NADH), dihydronicotinamide adenine dinucleotide phosphate tetrasodium salt (NADPH) were purchased from Bidepharm. 5-fluorouracil was purchased from Solarbio. Paclitaxel injection was purchased from Harbin Pharmaceutical Group Co., Ltd. Tetrabutylammonium hexafluorophosphate was purchased from Aladdin. 3-(4,5-dimethylthiazol-2-yl)-2,5-diphenyltetrazolium bromide (MTT) was purchased from MP Biomedicals. Human lung carcinoma cell line (A549), 5-FU-resistant human lung adenocarcinoma cell line (A549/5-FU) were obtained from ATCC, DDP-resistant human lung adenocarcinoma cell line (A549/DDP) and Paclitaxel-resistant human lung adenocarcinoma cell line (A549/PTX) were obtained from Procell Life Science&Technology Co.,Ltd. Dulbecco Modified Eagle Medium (DMEM), fetal bovine serum (FBS), penicillin/streptomycin and phosphate buffered saline (PBS) were bought from Gibco. Mito Tracker™ Green FM, Lyso Tracker™ Green DND-26 and MitoSOX™ Red mitochondrial superoxide indicator were purchased from Life Technologies Corporation. Mitochondrial membrane potential assay kit with JC-1, Annexin V-FITC/PI Apoptosis Detection Kit and Dihydroethidium (DHE) and ATP Assay Kit were purchased from Beyotime Biotechnology. Singlet oxygen sensor green reagent (SOSG) was purchased from meilunbio®. NADP/NADPH-Glo™ Assay product was purchased from Promega.

Instruments

^{1}H NMR spectra were recorded on Bruker Advance III. ^{1}H-^{1}H COSY and ^{13}C NMR spectra were recorded on 500MHz Bruker Advance III. Positive ion high resolution mass spectra were obtained by LCMS-IT-TOF (Shimadzu, Japan). UV-Visible absorption spectra were recorded on a double beam UV-vis spectrophotometer (YOUKE, T3202S). The fluorescence spectra and emission quantum yield measurements were measured on a Techcomp FL970 fluorescence spectrophotometer. The nanosecond transient absorption spectra were measured on an laser flash photolysis spectrometer (LP980, Edinburgh Instruments, Ltd., U.K.). Cyclic voltammograms were carried out using PGSTAT302N electrochemical workstation (Metrohm, Netherlands). Confocal microscopy was done with a laser confocal microscopy (LCSM 880, Carl Zeiss, Göttingen, Germany).

Synthesis and characterization

Synthesis of 2-[6-(1,8-Naphthyridin-2-yl)-2-pyridyl]-1,8-naphthyridine (bnp): bnp was prepared following reported literature.[1] To a mixture of 2,6-diacetylpyridine (1.645 g, 10.1 mmol) and 2-aminonicotinaldehyde (2.457 g, 20.1 mmol) was added a solution of NaOH (0.477 g) in ethanol (100 mL). The mixture was refluxed for 12 h at room temperature overnight. A light-yellow precipitate was collected and washed with absolute ethanol. Yield: 3.238 g, 96.6%. ^{1}H NMR (400 MHz, Chloroform-d) δ 9.21 – 9.17 (m, 2H), 9.01 (d, J = 7.6 Hz, 4H), 8.40 (d, J = 8.5

Hz, 2H), 8.28 (dd, 2H), 8.13 (t, *J* = 7.7 Hz, 1H), 7.54 (dd, 2H).

Synthesis of 4'-(pyren-1-yl)-2,2':6',2''-terpyridine (tpy-pyren): tpy-pyren was prepared following reported literature.[2] To a 250 mL round-bottom flask was added 2-acetylpyridine (2.447 g, 20.2 mmol) and 1-pyrenecarboxaldehyde (2.310 g, 10.0 mmol) dissolved in 75 mL of ethanol. Then sodium hydroxide (1.169 g, 29.2 mmol) and 35 ml of ammonia were added to the reaction mixture (scheme S1) and heated at reflux for 24h. The resulting precipitate was filtered and washed with distilled water. The yellow precipitate was collected as product. Yield: 2.565 g, 59.2%. ^{1}H NMR (400 MHz, Chloroform-*d*) δ 8.81 – 8.72 (m, 4H), 8.72 – 8.67 (m, 2H), 8.28 – 8.17 (m, 4H), 8.15 – 8.11 (m, 3H), 8.05 (d, *J* = 12.4 Hz, 2H), 7.92 (d, *J* = 1.7 Hz, 2H), 7.36 (ddd, *J* = 7.5, 4.7, 1.2 Hz, 2H).

Synthesis of Ru(tpy)Cl$_3$: To a mixture of 2,2':6',2"-terpyridine (2 mmol) and $RuCl_3 \cdot 3H_2O$ (2.1 mmol) were heated to 90 ℃ in ethanol for 4 hours. After distilled under reduced pressured and washed by water, a dark solid was prepared.

Synthesis of Ru(tpy-pyren)Cl$_3$: A mixture of $RuCl_3 \cdot 3H_2O$ (1.6 mmol) and 4'-(pyren-1-yl)-2,2':6',2''-terpyridine (1.7 mmol) were reacted in ethoxyethanol (150 mL) at 85 ℃ overnight. After cooling down to room temperature, the red-brown precipitate of Ru(tpy-pyren)Cl_3 was collected by filtration and washed by water to obtain a red-brown solid.

Synthesis of [Ru(tpy)$_2$](PF$_6$)$_2$ (Ru1): **Ru1** was prepared following reported literature.[3] To a mixture of 2,2':6',2''-terpyridine (0.117 g, 0.503 mmol) and ruthenium(III) chloride hydrate (0.057 g, 0.276 mmol) was added 1 mL of triethylamine. The reaction was heated to 120 ℃ for 20 h. Saturated ammonium hexafluorophosphate solution was followed added to the reaction mixture. The resulting solid was filtered and dry in vacuum. The crude product obtained was purified by column chromatography on neutral alumina (eluent: acetonitrile/dichloromethane = 2/1). The second band was collected, distilled and dried to obtain orange powders (0.110 g, yield 46.5%). HR-ESI-MS (MeOH): $[M\text{-}2PF_6]^{2+}$ calcd for $[C_{30}H_{22}RuN_6]^{2+}$: 284.0466, found: 284.0473. ^{1}H NMR (400 MHz, DMSO-d_6) δ 9.09 (d, *J* = 8.2 Hz, 4H, H_b), 8.83 (d, *J* = 8.1 Hz, 4H, H_c), 8.54 (t, *J* = 8.1 Hz, 2H, H_a), 8.02 (t, *J* = 8.0 Hz, 4H, H_d), 7.43 (d, *J* = 4.0 Hz, 4H, H_f), 7.26 (t, *J* = 8.0 Hz, 4H, H_e). ^{13}C NMR (500 MHz, DMSO-d_6) δ 157.73, 154.77, 152.08, 138.09, 135.88, 127.75, 124.53, 124.00.

Synthesis of [Ru(bnp)(tpy)](PF$_6$)$_2$ (Ru2): Ru2 was synthesized according to the previously reported method.[4] Ru(tpy)Cl_3 (0.6 mmol) and 2-[6-(1,8-Naphthyridin-2-yl)-2-pyridyl]-1,8-naphthyridine(bnp) (0.66 mmol) in ethylene glycol (15 mL) at 120 ℃ overnight. Then the mixture was cooled to room temperature, followed by addition of saturated aqueous solution of NH_4PF_6. The crude product of **Ru2** was collected by filtration and washed by water**,** purified by neutral alumina column chromatography using 3: 1 mixture of acetonitrile: dichloromethane as the eluent and obtained as purple solid. Yield: 0.168 g, 29.1%. HR-ESI-MS (MeOH): $[M\text{-}2PF_6]^{2+}$ calcd for $[C_{36}H_{24}RuN_8]^{2+}$: 335.0579, found: 335.0583. ^{1}H NMR (400 MHz, DMSO-d_6) δ 9.48 (d, *J* = 8.2 Hz, 2H, H_b), 9.10 (d, *J* = 8.6 Hz, 2H, H_i), 9.02 (d, *J* = 8.1 Hz, 2H, H_h), 8.73 (d, *J* = 8.4Hz, 2H, H_j), 8.71 (t, *J* = 8.4 Hz, 1H, H_a), 8.62 (d, *J* = 8.0

Hz, 2H, H_c), 8.61 (t, J_2 = 8.0 Hz, 1H, H_g), 8.42 (d, J = 6.9 Hz, 2H, H_m), 8.21 (d, J = 2.7 Hz, 2H, H_k), 7.80 (t, J = 7.8 Hz, 2H, H_d), 7.56 (dd, J = 4.0 Hz, 2H, H_l), 7.35 (d, J = 5.6 Hz, 2H, H_f), 7.05 (t, J_2 = 4.0 Hz, 2H, H_e). ^{13}C NMR (500 MHz, DMSO-d_6) δ 162.31, 160.29, 157.04, 156.75, 156.04, 154.22, 153.15, 140.63, 139.07, 138.29, 135.81, 135.30, 127.29, 127.06, 124.89, 124.46, 123.64, 122.41, 121.58.

Synthesis of [Ru(bnp)(tpy-pyren)](PF$_6$)$_2$ (Ru3): Ru3 was obtained by refluxing Ru(tpy-pyren)Cl_3 (0.6 mmol) and 2-[6-(1,8-Naphthyridin-2-yl)-2-pyridyl]-1,8-naphthyridine(bnp) (0.385 g, 0.665 mmol) in 2-Ethoxyethanol (6 mL) at 120 ℃ overnight. After the reaction, the mixture was cooled to room temperature, followed by addition of saturated aqueous solution of NH_4PF_6. The crude precipitate of [Ru(bnp)(tpy-pyren)](PF$_6$)$_2$ was collected by filtration and washed by water. The crude product obtained was purified by column chromatography on neutral alumina (eluent: acetonitrile/dichloromethane = 1/1). The forth band was collected and distilled under reduced pressure to obtain purple solid. Yield: 0.210 g, 30.0%. HR-ESI-MS (MeOH): $[M\text{-}2PF_6]^{2+}$ calcd for $[C_{52}H_{32}RuN_8]^{2+}$: 435.0893, found: 435.0898. ^{1}H NMR (400 MHz, DMSO-d_6) δ 9.52 (d, J = 8.2 Hz, 2H, H_b), 9.39 (s, 2H, H_b), 9.15 (d, J = 8.7 Hz, 2H, H_i), 8.80 – 8.71 (m, 7H, $H_{c,g,j,s,r}$), 8.62 – 8.42 (m, 10H, $H_{k,m,n,o,p,q,u,t}$), 8.24 (t, J = 7.6 Hz, 1H, H_a), 7.79 (t, J = 7.8 Hz, 2H, H_d), 7.69 (dd, J = 8.0, 4.2 Hz, 2H, H_l), 7.43 (d, J = 5.6 Hz, 2H, H_f), 7.09 (t, J = 6.6 Hz, 2H, H_e). ^{13}C NMR (500 MHz, DMSO-d_6) δ 162.41, 160.36, 157.05, 156.85, 156.17, 154.34, 153.24, 148.13, 140.76, 139.18, 138.31, 135.43, 134.38, 132.02, 131.54, 130.95, 129.78, 128.96. δ 128.66, 127.99, 127.46, 127.40, 127.15, 126.66, 126.14, 125.78, 125.19, 124.75, 124.61, 124.50, 124.35, 124.12, 123.90, 121.69, 63.27.

High Performance Liquid Chromatography (HPLC) analysis

Ru1 and **Ru3** HPLC analysis was performed on an Agilent 1260 Infinity II Prime system. **Ru2** was performed on Shimadzu LC system. **Ru1-Ru3** was dissolved in HPLC grade acetonitrile to give a complex concentration of 50 μM. The complexes were analyzed by reversed-phase Agilent ZORBAX SB-C18 column (4.6*250 mm) at 25 ℃ with a flow rate of 1 mL/min and UV-detector was set at 308, 365, 312 nm, respectively. The solvent system consists of two eluents: mobile phase A was water/acetonitrile/formic acid (950//50/1, v/v/v) while mobile phase B was acetonitrile/formic acid (1000/1, v/v/v). The procedure run with a gradient: 0.01 min (5% phase B), 20 min (100% phase B). All samples were analyzed using the same method.

UV-Visible absorption spectra

The UV-Vis spectra of the complexes were recorded by a double beam UV-vis spectrophotometer (YOUKE, T3202S) with 1-cm path-length quartz cuvettes, and the obtained data was processed using Origin software. The UV-Visible spectra absorption measurement of **Ru1-Ru3** (10 μM) experiments were carried out at 298 K from 800 to 300 nm.

Phosphorescence spectra

Phosphorescence emission measurements were performed on a Techcomp FL970 fluorescence spectrophotometer. The complexes of **Ru1-Ru3** (10 μM) in eight different solvents were excited at λ_{ex} = 635 nm and in a 1-cm quartz cuvette at 298 K. The hypoxia photoluminescence spectra of **Ru1-Ru3** (10 μM) in acetonitrile (CH_3CN) were obtained after purging N_2 into the solution for 5

min before excited at 635 nm. The incident slit and exit slit were set as 10 nm.

Measurement of lipo-hydro partition coefficient

Mixture of n-octanol and water (1:1 v/v, 20 mL) was shook for 24 h by a constant temperature oscillator so that the two phases can be saturated with each other. The **Ru1-Ru3** were added to a mixture of 1 mL water-saturated n-octanol and 1 mL n-octanol saturated water to reach the final concentration of 50 μM. The solution was mixed and then shook up at speed of 200 r/min on a constant temperature oscillator for overnight. After stationary, the two-phases were dispersed in 2 mL ethanol, respectively, and then the complex concentration in each phase was quantified by measuring the absorbance at 500 nm. The calculation formula: log Po/w = log (C_o/C_w) =log (the concentration of complex in octanol phase / the concentration of complex in water phase).

Photoluminescence quantum yield and lifetime measurements

Photoluminescence spectra were obtained with a fluorescence spectrophotometer. The relative photoluminescence quantum yields were determined with MB as the standard using the following equation:

$$\Phi_x = \Phi_s * (F_x/F_s) * (A_s/A_x) * (n_x/n_s)^2$$

Where Φ represents quantum yield; F stands for integrated area under the corrected emission spectrum; A is absorbance at 635 nm, the excitation wavelength; n is the refractive index of the solution; and the subscripts x and s refer to the complex sample and the standard, respectively. **Ru2-Ru3** were diluted from a stock solution in DMSO to achieve an absorbance = 0.1 at 635 nm in water or acetonitrile. The Φ_p value for MB in aerated water and acetonitrile at 298 K were measured to be 0.01 and 0.08 respectively. These values for the phosphorescence quantum yield of MB have been reported in previous literatures.[5]

Nanosecond transient absorption spectra

The nanosecond transient absorption spectra and triplet excited-state lifetime were recorded on LP980 laser flash photolysis spectrometer (Edinburg Instruments, Ltd., UK). All samples (10 μM) were dissolved in CH_3CN and deaerated with Ar for ca. 15 min before measurement, then excited with a nanosecond pulsed laser (Opolette 355II+UV nanosecond pulsed laser. OPOTEK) at 355 nm (5 mJ per pulse). The data of kinetic decay trace and curve fitting were analyzed with L900 software.

Dark- and photo- stability study

Dark- and photo- stability study were analyzed by ^{1}H NMR spectra and UV-Vis absorption spectra. The solution experiment was carried out in DMEM solution free of phenol red at ambient temperature. For the dark-stability experiment, **Ru1-Ru3** (30 μM) were kept in the dark and recorded UV-Vis absorption spectra at 0, 12, 24 h, respectively. For the photo-stability experiment, DMEM solution of **Ru1-Ru3** (30 μM)**,** methyl blue (30 μM**)** and chlorin e6 (10 μM) were recorded UV-Vis spectra every five minutes after light irradiation (635 nm, 23.59 mW/cm^2). The ^{1}H NMR spectra of **Ru1-Ru3** in DMSO-d_6 was conducted at 298K after 48 h in the dark or light irradiation (635 nm, 63.7 J/cm^2).

Cyclic voltammetry

The electrochemical properties of **Ru1**-**Ru3** were studied using cyclic voltammetry (CV) with a common three electrode system: a glassy-carbon is the working electrode, a platinum wire is the counter electrode, and Ag/AgCl in saturated KCl solution is the reference electrode. All electrochemical measurements were recorded in degassed HPLC grade acetonitrile containing 0.1 M Bu_4NPF_6 used as conducting salt and the concentration of the complexes was ~1 mM. All data were referenced versus the Fc^+/Fc redox potential (set as 0 V in the cyclic voltammograms). Voltammograms were scanned from -1.6 V to +1.6 V (three complete scans for each experiment to ensure reproducibility).

Computational details

All the calculations of complexes were performed by using the Gaussian 16 package[6]. The ground state geometry optimizations and spin density isosurfaces of the complexes were calculated by using density functional theory (DFT) method with the optimized ground state and triplet state geometries, respectively. Geometry optimizations were performed by using the PBE0 exchange-correlation functional (XC) with the 6-31 G (d,p) basis set to describe all atoms except the Ru (II) metal ion, which was described using the quasi-relativistic Stuttgart-Dresden (SDD) pseudopotential.[7]

The energy levels and orbitals of the singlet and triplet excited states calculations were performed by using time-dependent density functional theory (TD-DFT) method. The calculations were carried out by using Becke's three parametrized Lee-Yang-Parr (B3LYP) exchange correlation functional with the SDD effective core potential for Ru (II) and 6-31G (d,p) basis sets for the other atoms,[8] to explore the effects of the solvent environment, the integral equation formalism polarizable continuum model (IEFPCM) was adopted. The natural transition orbitals (NTOs) analysis was carried out by utilizing electronic wavefunction analysis software, Multiwfn 3.8 and VMD.[9,10]

Photocatalytic reactions of Ru^{II} complexes with NAD(P)H

UV-Vis spectra

Reactions between **Ru1**-**Ru3** (5 μM) and NAD(P)H in PBS at different ratios were monitored by UV-Vis spectroscopy at 298 K in the dark or on irradiation with 635 nm (27.08 mW/cm^2) light. The concentration NADH and NADPH was obtained by using the extinction coefficient ε_{339} = 6220 $M^{-1}cm^{-1}$ (NADH) and ε_{339} = 6300 $M^{-1}cm^{-1}$. The turnover number of catalysis was calculated using the following equations:

$$[NAD(P)^+] = [Abs(339\ nm)_{initial}\text{-}Abs(339\ nm)_{final}]/Abs(339\ nm)_{initial}*[NAD(P)H]$$

$$\text{Turnover number (TON)} = [NAD(P)^+]/[\text{Catalyst}]$$

$$\text{Turnover frequency (TOF)} = \text{Turnover number/time (h)}$$

Detection of H_2O_2 generation

For the reaction of complexes **Ru1**-**Ru3** (50 μM) with NAD(P)H in the PBS solution at 298 K in the dark or after irradiation for 30 min (635 nm, 42.5 J/cm^2), H_2O_2 was detected by EasyBox® hydrogen peroxide test sticks (HuanKai Microbial). The H_2O_2 generation level of the solution could be shown by the color from white to blue of test sticks indicating 0-25 mg/L H_2O_2.

Detection of intracellular NADPH and ATP level

1×10^4 A549/DDP cells were seeded per well in 96-well plates in incubator for 24 h. Then the cells were treated with different concentration of **Ru3** for 4 h. After this, supernatants were removed and each well was washed with PBS for twice. For light treatment, the cells were then irradiated with red light (635 nm, 63.7 J/cm^2). The NADP/NADPH-Glo™ Assay product (Promega) and ATP Assay Kit (Beyotime) were used to measure the intracellular NADPH and ATP level. The luminescence was recorded using a microplate reader. Three replicates were set for each sample, and the standard deviations were calculated in each group.

Determination of singlet oxygen generation

The production of singlet oxygen ($^1O_2$) in solution was detected using 9, 10-anthracenediyl bis(methylene) dimalonic acid (ABDA) as $^1O_2$ probe. **Ru1-Ru3** (10 μM) in PBS was mixed with ABDA (200 μM). The reaction mixture was taken in a quartz cuvette and the absorbance of ABDA was monitored by UV-vis at 298 K after 635 nm (27.08 mW/cm^2) light irradiation for different interval.

The $^1O_2$ generation quantum yield (Φ_Δ) of **Ru2-Ru3** were evaluated by indirect method. **Ru2-Ru3** and MB were diluted in PBS to reach around 0.1 absorbance at 635 nm and added with ABDA (200 μM). The absorption of ABDA at 380 nm were recorded every 30 s. The $^1O_2$ generation quantum yields were determined with MB ($\Phi_{\Delta s}$ = 0.52 in aqueous solution)[11] as the standard using the following equation:

$$\Phi_{\Delta x} = \Phi_{\Delta s} * (S_x/S_s) * (F_s/F_x)$$

Where Φ_Δ represents $^1O_2$ generation quantum yield; subscripts x and s designate the sample and MB, respectively; S stands for the slope of plot matching difference value of absorbance against the irradiation time (s); F stands for the absorption correction factor, which is calculated by $F = 1 - 10^{-OD}$ (OD represents the optical density of sample and MB at 635 nm).

Cell culture

Cell lines A549, A549/DDP, A549/PTX, A549/5-FU were maintained in DMEM medium supplemented with 10% fetal bovine serum, and 1% penicillin-streptomycin solution. All cells were grown at 310 K in a humidified incubator which provided an atmosphere of 5 % CO_2. According to the standard of cell STR authentication established by the International Cell Authentication Committee (ICLAC), they were considered derived from a common ancestral cell while the matching degree of cell lines with database was ≥ 80%.

STR profile of A549 and A549/5-FU cells

A549		A549/5-FU	
STR Loci	Result	STR Loci	Result
Amelogenin	X，Y	**Amelogenin**	X，Y
CSF1PO	10,12	**CSF1PO**	10,12
D13S317	11	**D13S317**	11
D16S539	11,12	**D16S539**	11,12

D18S51	14，17	**D18S51**	14，17
D19S433	13	**D19S433**	13
D21S11	29	**D21S11**	29
D2S1338	24	**D2S1338**	24
D3S1358	16	**D3S1358**	16
D5S818	11	**D5S818**	11
D7S820	8，11	**D7S820**	8，11
D8S1179	13，14	**D8S1179**	13，14
FGA	23	**FGA**	23
TH01	8，9.3	**TH01**	8，9.3
TPOX	8，11	**TPOX**	8，11
vWA	14	**vWA**	14

STR profile of A549/DDP and A549/Tax cells

A549/DDP		A549/PTX	
STR Loci	Result	STR Loci	Result
Amelogenin	X,Y	**Amelogenin**	X,Y
CSF1PO	10,12	**CSF1PO**	10,12
D2S1338	24	**D2S1338**	24
D3S1358	16	**D3S1358**	16
D5S818	11	**D5S818**	11
D7S820	8,11	**D7S820**	8,11
D8S1179	13,14	**D8S1179**	13,14
D13S317	11	**D13S317**	11
D16S539	11,12	**D16S539**	11,12
D18S51	14,17	**D18S51**	14,17
D19S433	13	**D19S433**	13
D21S11	29	**D21S11**	29
FGA	23	**FGA**	23
PentaD	9	**PentaD**	9
PentaE	7,11	**PentaE**	7,11
TH01	8,9.3	**TH01**	8,9.3
TPOX	8,11	**TPOX**	8,11
vWA	14	**vWA**	14
D6S1043	11,13	**D6S1043**	11,13
D12S391	18	**D12S391**	18
D2S441	10,13	**D2S441**	10,13

MTT cytotoxicity assay

Cell viability was determined by MTT assay and performed in triplicate in 96-well plates. Cells were maintained in DMEM with 10% FBS and 1% penicillin-streptomycin solution. 100 μL warm culture medium containing about 5×10^3 cells were seeded per well in 96-well plates, and placed in a 37 ℃, 5% CO_2 incubator for 24 h to achieve cell attachment. After that, the medium was removed completely, the fresh medium containing different concentrations of the compounds was added to each well. The final concentration of DMSO was lower than 0.1% (v/v). After incubation for 4 h, the medium was removed and was replaced by fresh medium. The dark groups were placed in the incubator for futher incubation, the light groups were irridated with 635 nm light (63.7 J/cm^2) followed by 44 h incubation. After that, MTT (10 μL, 5 mg/mL) was added to each well and incubated for another 4 h at 37 ℃. The medium was removed and DMSO (100 μL) was added to each well to dissolve the formed purple formazan. Then the optical density (OD) at 570 nm was measured with a microplate reader (Bio-TEK, USA).

Colocalization assays

A549/DDP cells were seeded in a confocal dish and cultured under favorable conditions. After 48 h, **Ru3** (50 μM) was added to incubate with the cells for 6 h and were further stained with Lyso- and Mito-Tracker (100 nM) for 30 min. Intracellular distribution was done by confocal microscope (LCSM 880, Carl Zeiss, Göttingen, Germany) with a 63× objective lens. **Ru3** was excited at 633 nm, Lyso- and Mito- Tracker were excited at 488 nm. The phosphorescence/fluorescence was collected at 700 ± 40 nm for **Ru3** and 550 ± 40 nm for Lyso- and Mito-Tracker.

Determination of intracellular reactive oxygen species

A549/DDP cells were seeded into 96-well plate at the density of 5000 cells per well and incubated for 48 h. After that, cells were incubated with **Ru3** (1 μM /2.5 μM) at 310 K for 2 h. The light groups then were on irradiation at 635 nm (63.7 J/cm^2) light. Further, cells were incubated with 10 μM Reactive Oxygen Species Assay Kit (DCFH-DA) at 310K for 30 min in the dark and washed once with PBS before observed by an inverted fluorescence microscope.

Determination of intracellular superoxide anion ($O_2^{\bullet-}$)

A549/DDP cells were seeded into 96-well plate at the density of 5000 cells per well and incubated for 48 h. After that, cells were incubated with **Ru3** (1 μM /2.5 μM) at 310 K for 2 h. The light groups then were on irradiation at 635 nm (63.7 J/cm^2) light. Further, cells were incubated with 5 μM dihydroethidium (DHE) at 310K for 30 min in the dark and washed once with PBS before observed by an inverted fluorescence microscope.

Determination of intracellular singlet oxygen ($^1O_2$)

A549/DDP cells were seeded into 96-well plate at the density of 5000 cells per well and incubated for 48 h. After that, cells were incubated with **Ru3** (1 μM /2.5 μM) at 310 K for 2 h. The light groups then were on irradiation at 635 nm (63.7 J/cm^2) light. Afterward, cells were incubated with 5 μM Singlet Oxygen Sensor Green Reagent (SOSG) at 310K for 30 min in the dark and washed once with PBS before observed by an inverted fluorescence microscope.

Mitochondrial membrane potentials ($\Delta\Psi_m$) assays

The mitochondrial membrane potential was determined by JC-1 dye. A549/DDP cells were seeded into 96-well plate at the density of 5000 cells per well and incubated for 48 h. After that, cells were incubated with **Ru3** (1 μM) at 310 K for 2 h. The light groups then were on irradiation at 635 nm (63.7 J/cm^2) light. Furthermore, cells were incubated in the dark at 310 K, 5% CO2 incubator for another 1h. Subsequently, cells were stained with JC-1 (2.5 μg/mL) at 310 K for 20 min in the dark and washed once with PBS. The cells were imaged by an inverted fluorescence microscope.

Detection of intracellular mitochondrial superoxide

A549/DDP cells were seeded into 96-well plate at the density of 5000 cells per well and incubated for 48 h. After that, cells were incubated with **Ru3** (1 μM) at 310 K for 2 h. The light groups then were on irradiation at 635 nm (63.7 J/cm^2) light. Furthermore, cells were incubated in the dark at 310 K, 5% CO2 incubator for another 1h. Afterward, cells were incubated with 5 μM MitoSOX™ red probe at 310K for 10 minutes in the dark and washed twice with PBS before observed by an inverted fluorescence microscope.

Annexin V-FITC/PI assays

Mode of cell death was detected by Annexin V-FITC/PI dual staining. A549/DDP cells were seeded into 96-well plate at the density of 5000 cells per well and incubated for 48 h. After that, cells were incubated with **Ru3** (1 μM) at 310 K for 2 h. The light groups then were on irradiation at 635 nm (63.7 J/cm^2) light. After that, Cells were stained with annexin V-FITC (2.5 μL) and PI (5 μL) stock solution in the dark for 15 min at ambient temperature. The fluorescence images were obtained within an hour on an inverted fluorescence microscope.

In vivo biocompatibility evaluation toward Zebrafish

Zebrafish experiments were carried out under Laboratory Animal Center, Sun Yat-sen University, Guangzhou, China. All animals were maintained in accordance with ASPA 1986. *Tg(flk1:EGFP)^{s843}* embryos[12] were used in this experiment. 24-well plates were prepared with several concentrations of **Ru3** complex (1 μM, 2.5 μM, 10 μM, blank control), eggs grown and developed normally were selected and randomly divided (3 eggs & 1 mL egg water containing methylene blue per well). Each well seed 1-3 embryos, incubated for 72 h (3 days) at 28±0.5 ℃ and monitored at least once a day. Light cycle: 14 hours day, 10 hours night. The situation of embryos was observed by a microscopy.

Cellular metabolomics study

Sample preparation

A549/DDP cells were seeded in 6 cm dishes (Corning) and cultured for 48 h. Six replicate samples were set for each group treated with:

(1) **D**: 1% (v/v) DMSO,

(2) **L**: 1% (v/v) DMSO + Laser (635 nm, 63.7 J/cm^{-2}),

(3) **Ru3**-D: Only **Ru3** (0.2 μM),

(4) **Ru3**-L: **Ru3** (0.2 μM) + Laser (635 nm, 63.7 J/cm^{-2}).

After corresponding treatment for 4 h, the medium was removed and replaced by fresh medium.

The **D** and **Ru3-**D groups were placed in the dark for 1 h at 37 ℃ in a 5% CO_2 humidified incubator, the **L** and **Ru3-**L groups were irridated with 635 nm light (63.7 J/cm^2) and continue to be incubated for 1 h. The cells were trypsinized, washed three times with cold PBS and counted $1*10^6$ cells for each sample. Centrifuged cells were taken and placed in a 1.5 mL EP tube and quenched in liquid nitrogen for at least 30 s and then stored at −80 °C in ultra-low temperature freezer previous to testing.

Metabolites Extraction

The LC/MS system for metabolomics analysis is composed of Waters Acquity I-Class PLUS ultra-high performance liquid tandem Waters Xevo G2-XS QTof high resolution mass spectrometer. The column used is purchased from Waters Acquity UPLC HSS T3 column (1.8um 2.1*100mm)

The mobile phase A was 0.1% formic acid aqueous solution, and the mobile phase B was 0.1% formic acid acetonitrile. The injection volume of samples was 1 μL. Both positive ion mode and negative ion mode were conducted under the same condition.

LC-MS/MS Analysis

Waters Xevo G2-XS QTOF high resolution mass spectrometer can collect primary and secondary mass spectrometry data in MSe mode under the control of the acquisition software (MassLynx V4.2, Waters). In each data acquisition cycle, dual-channel data acquisition can be performed on both low collision energy and high collision energy at the same time. The low collision energy is 2V, the high collision energy range is 10~40V, and the scanning frequency is 0.2 seconds for a mass spectrum. The parameters of the ESI ion source are as follows: Capillary voltage: 2000V (positive ion mode) or -1500V (negative ion mode); cone voltage: 30V; ion source temperature: 150 ℃; desolvent gas temperature 500 ℃; backflush gas flow rate: 50L/ h; Desolventizing gas flow rate: 800L/h.

Data preprocessing and annotation

The raw data collected using MassLynx V4.2 is processed by Progenesis QI software for peak extraction, peak alignment and other data processing operations, based on the Progenesis QI software online METLIN database and Biomark's self-built library for identification, and at the same time, theoretical fragment identification and mass deviation All are within 100ppm.

General clustering trends and metabolite differences were assessed with principal component analysis (PCA). Metabolite variations and reliability of models (R2Y and Q2~1) were confirmed with supervised orthogonal partial least square discriminant analysis (OPLS-DA). According to Fold Change (FC > 1), VIP value (VIP > 1) obtained by OPLS-DA model and p value obtained by t test ($p < 0.05$), the most unique metabolites were identified by Venn diagram.

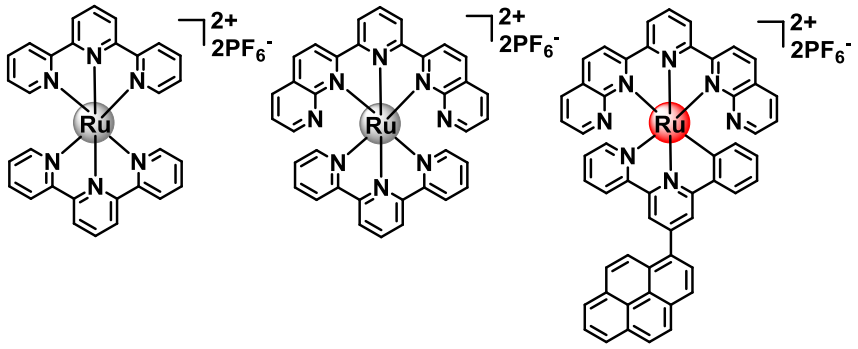

Scheme S1. Structure of complexes **Ru1-Ru3**.

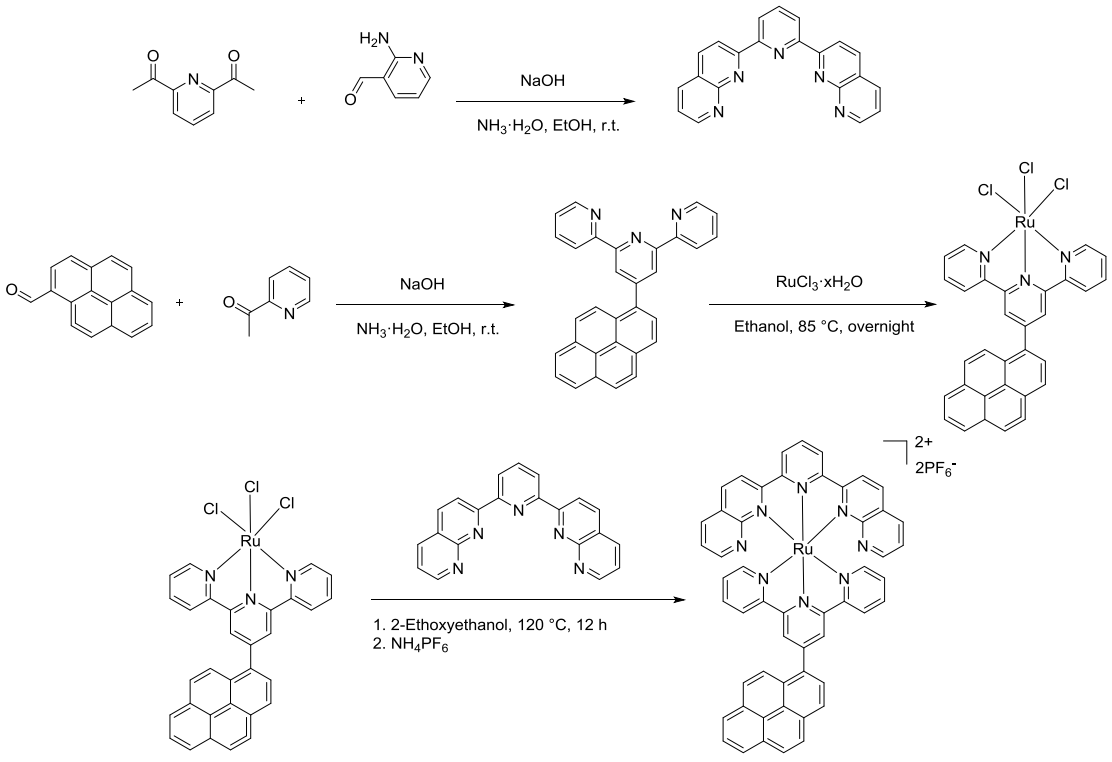

Scheme S2. Synthetic scheme for complex **Ru3**.

Figures

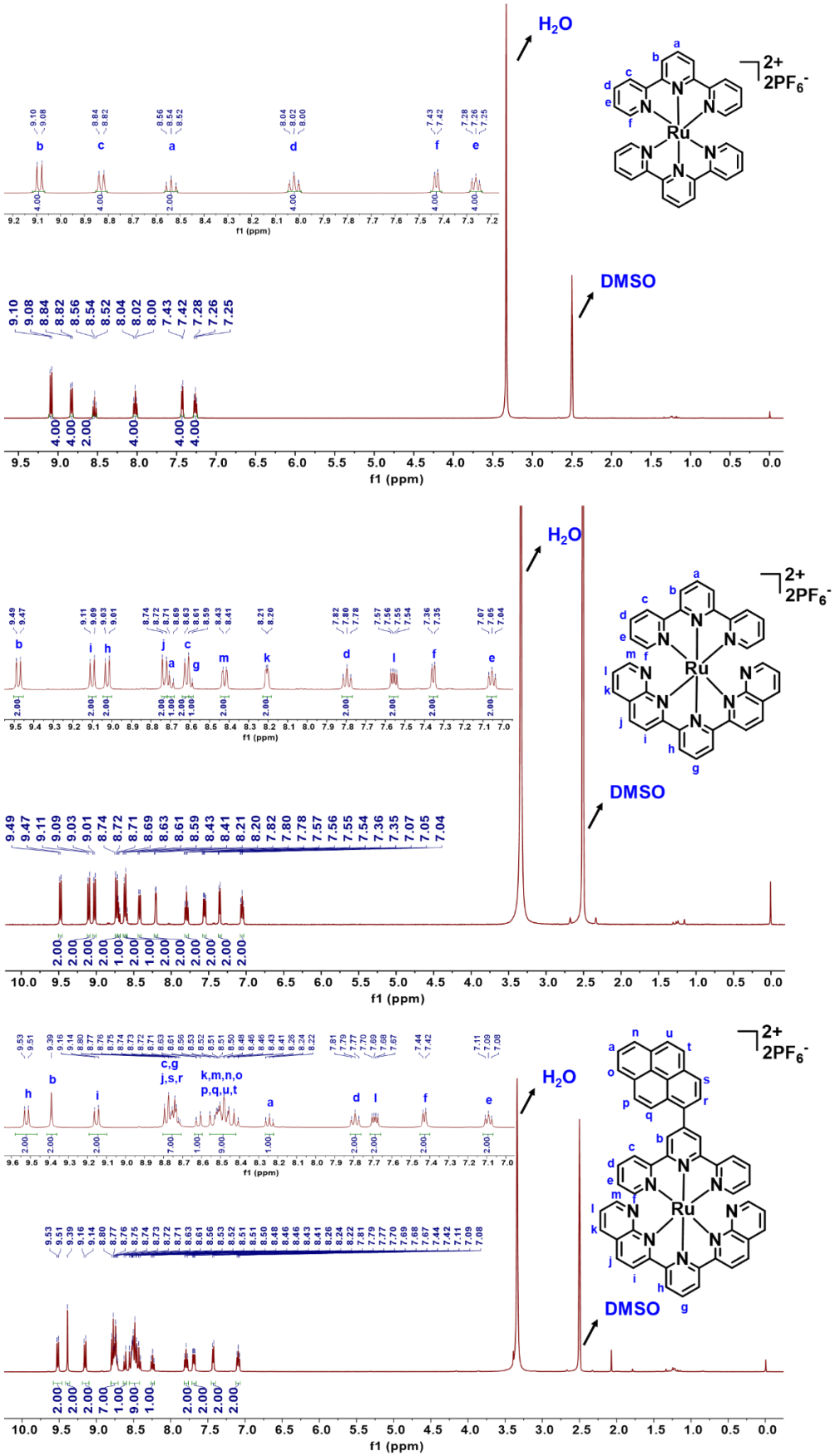

Figure S1. ^{1}H NMR spectra (400 MHz, DMSO-d_6) of **Ru1**-**Ru3**.

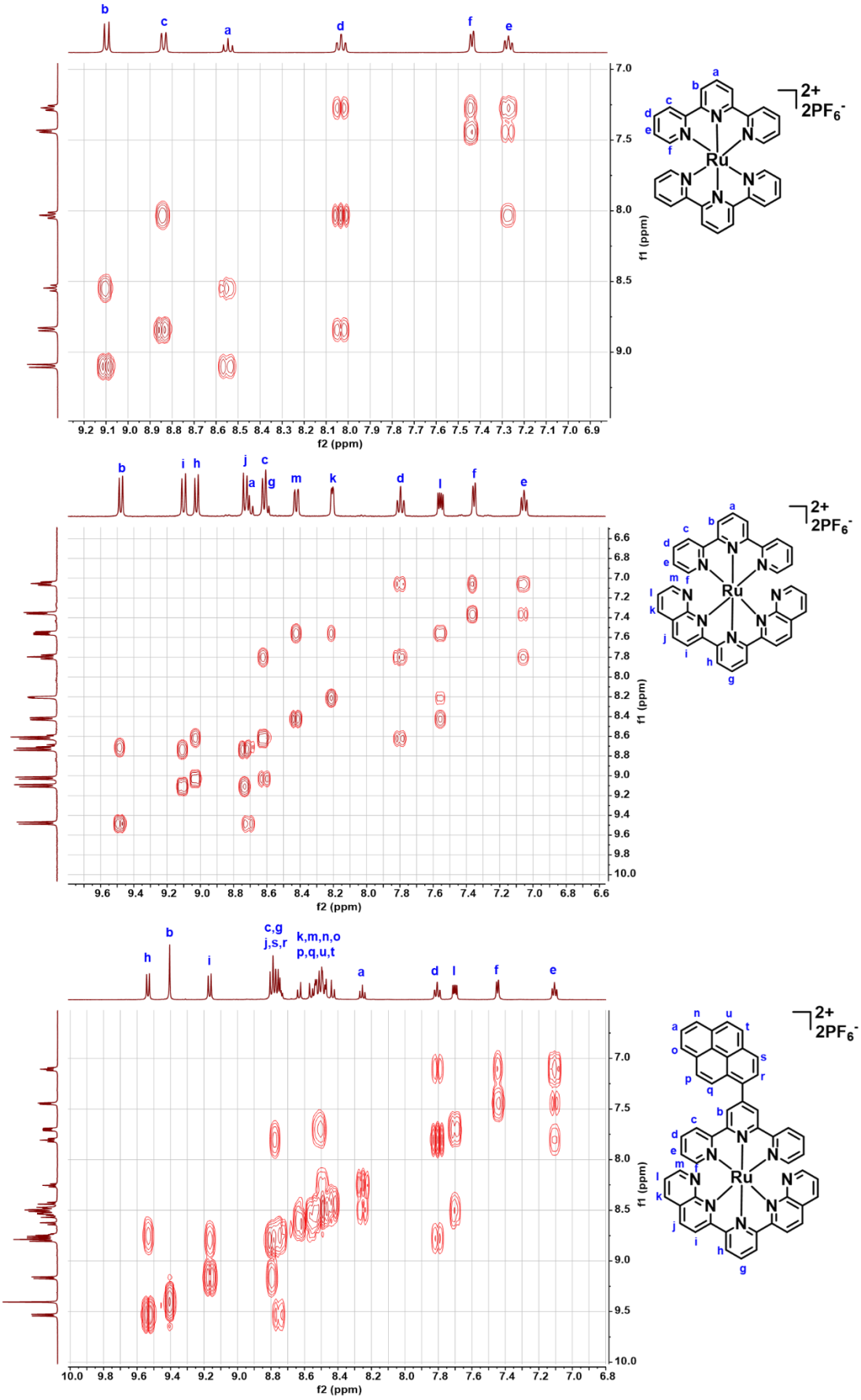

Figure S2. ^{1}H-^{1}H COSY spectra (500 MHz, DMSO-d_6) of **Ru1-Ru3**.

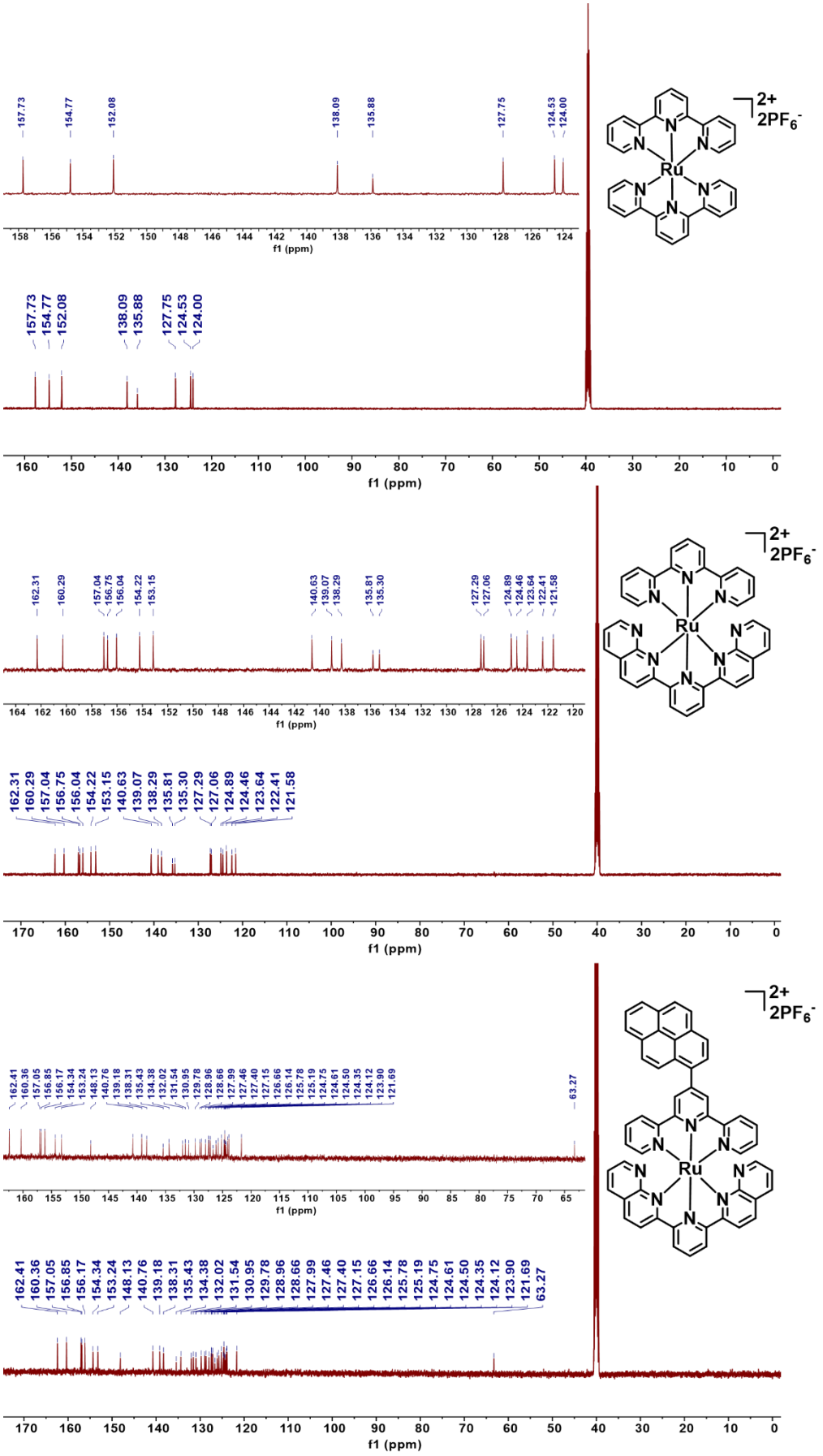

Figure S3. ^{13}C NMR spectra (500 MHz, DMSO-d_6) of **Ru1-Ru3**.

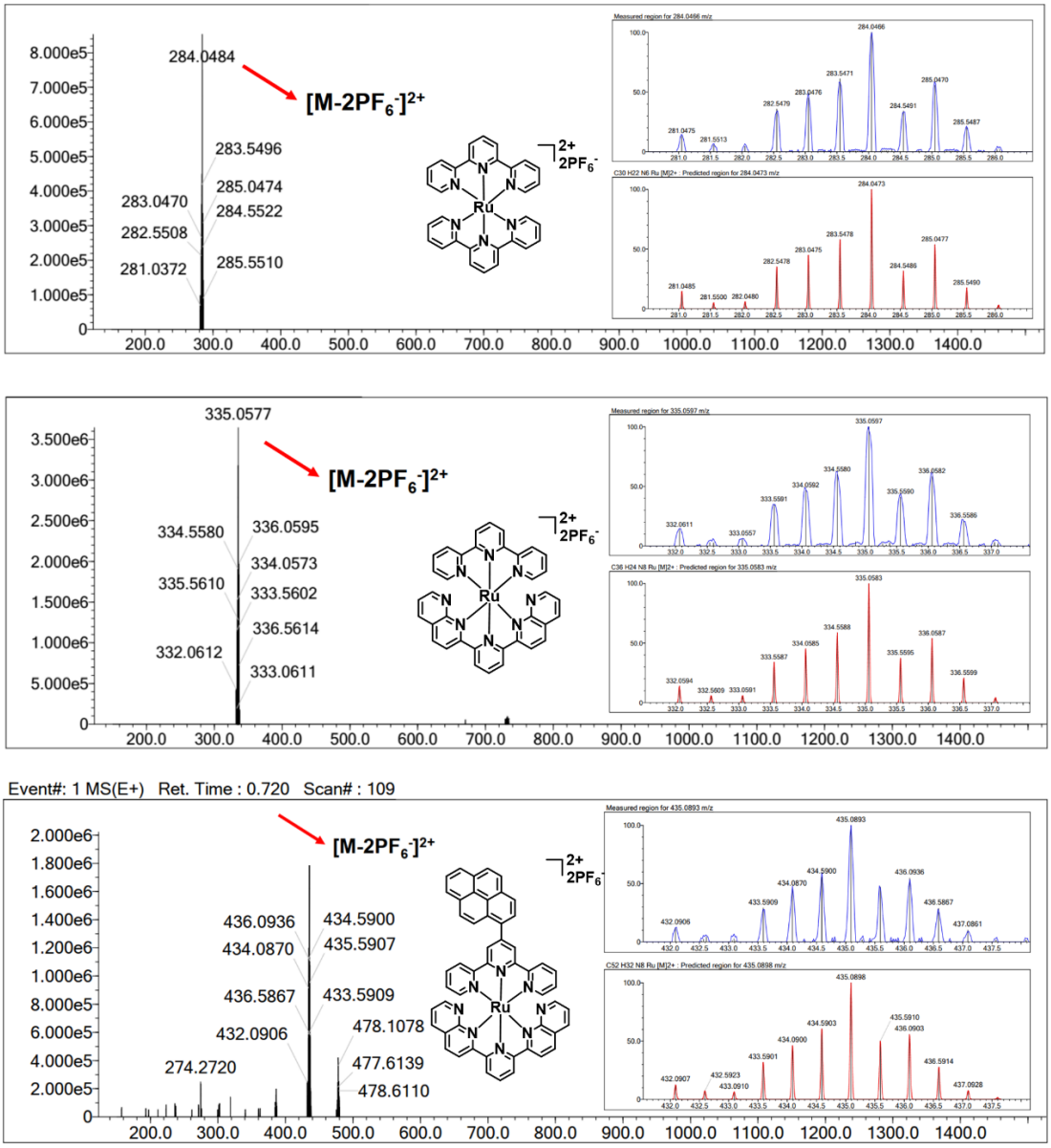

Figure S4. HR-ESI-MS spectra of **Ru1**-**Ru3**.

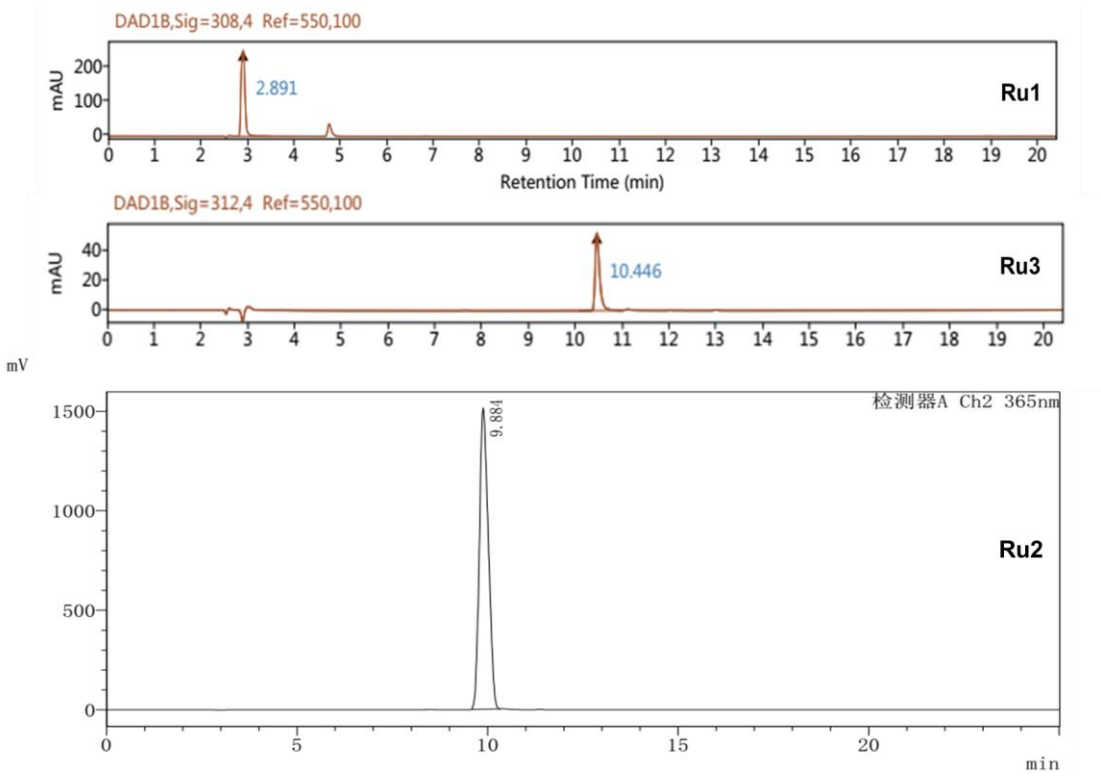

Figure S5. HPLC spectra of **Ru1**-**Ru3**.

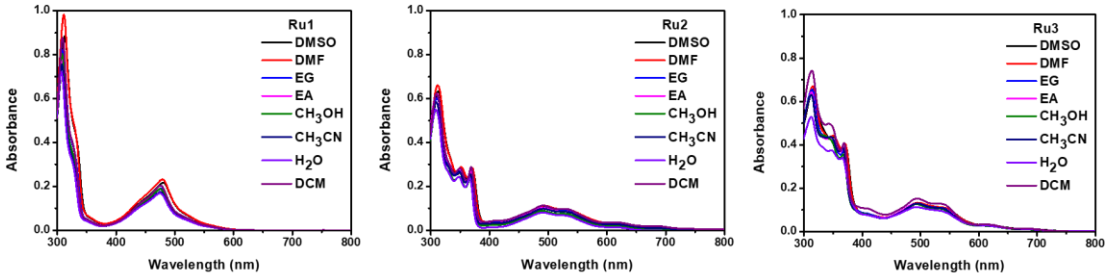

Figure S6. UV-vis spectra of **Ru1**-**Ru3** (10 μM) in different solvents.

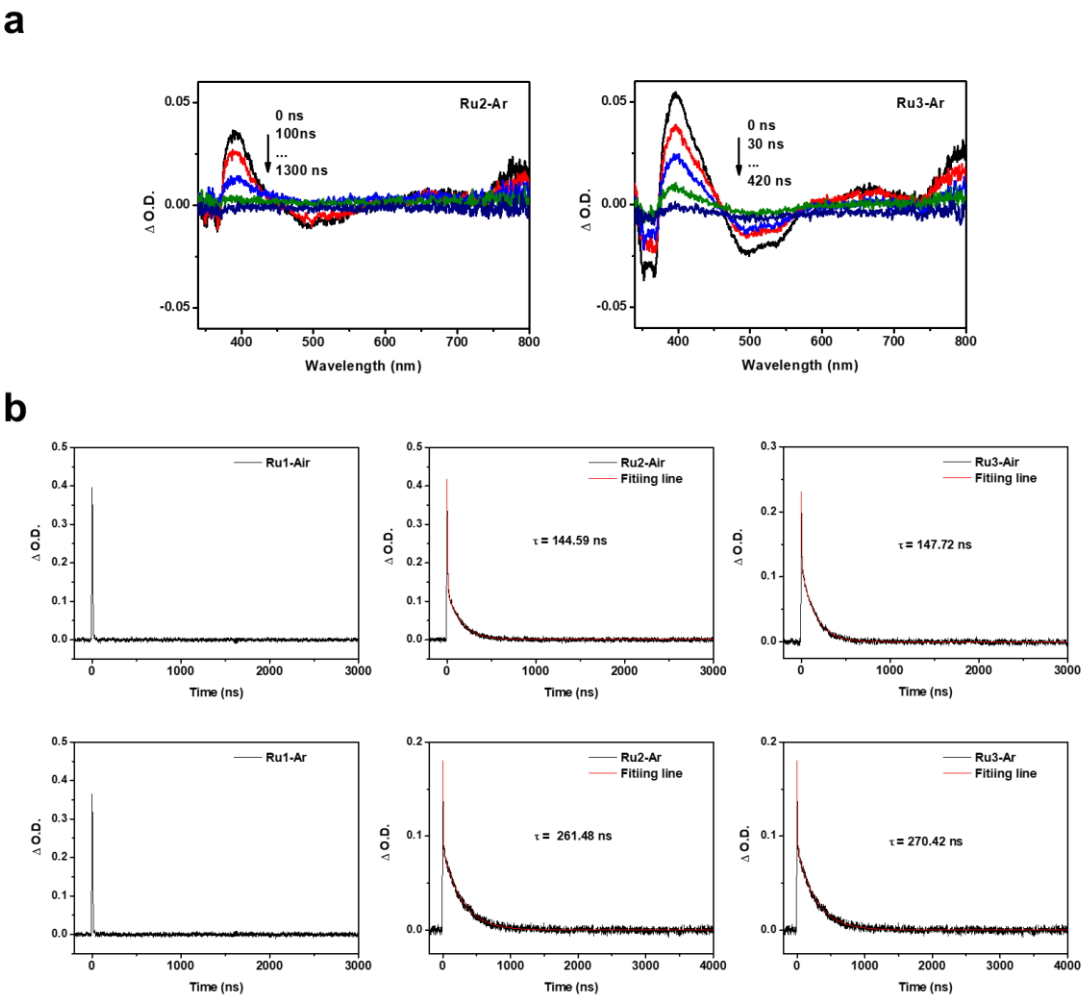

Figure S7. (a) Time-resolved transient spectra of **Ru2** and **Ru3** (10 μM) in deaerated CH_3CN after pulsed excitation, λ_{ex} = 355 nm. (b) Decay traces of the triplet excited-state lifetime of Ru(II) complexes***** at 310 nm in deaerated CH_3CN.

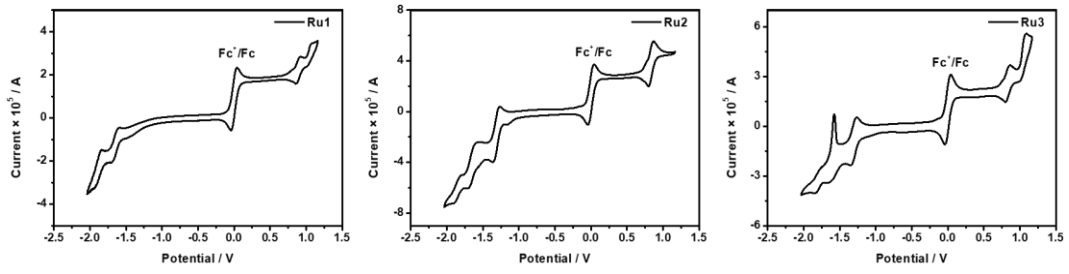

Figure S8. Cyclic voltammogram of the complexes **Ru1**-**Ru3** in deaerated CH_3CN. Potentials are referenced to Ag/AgCl in saturated KCl solution as the reference electrode via an internal ferrocene standard (set as 0 V in the cyclic voltammograms). 0.1 M Bu_4NPF_6 was used as the supporting electrolyte; Scan rate = 100 mV/s; c = 1.0 × 10^{-3} M; T = 25 ℃.

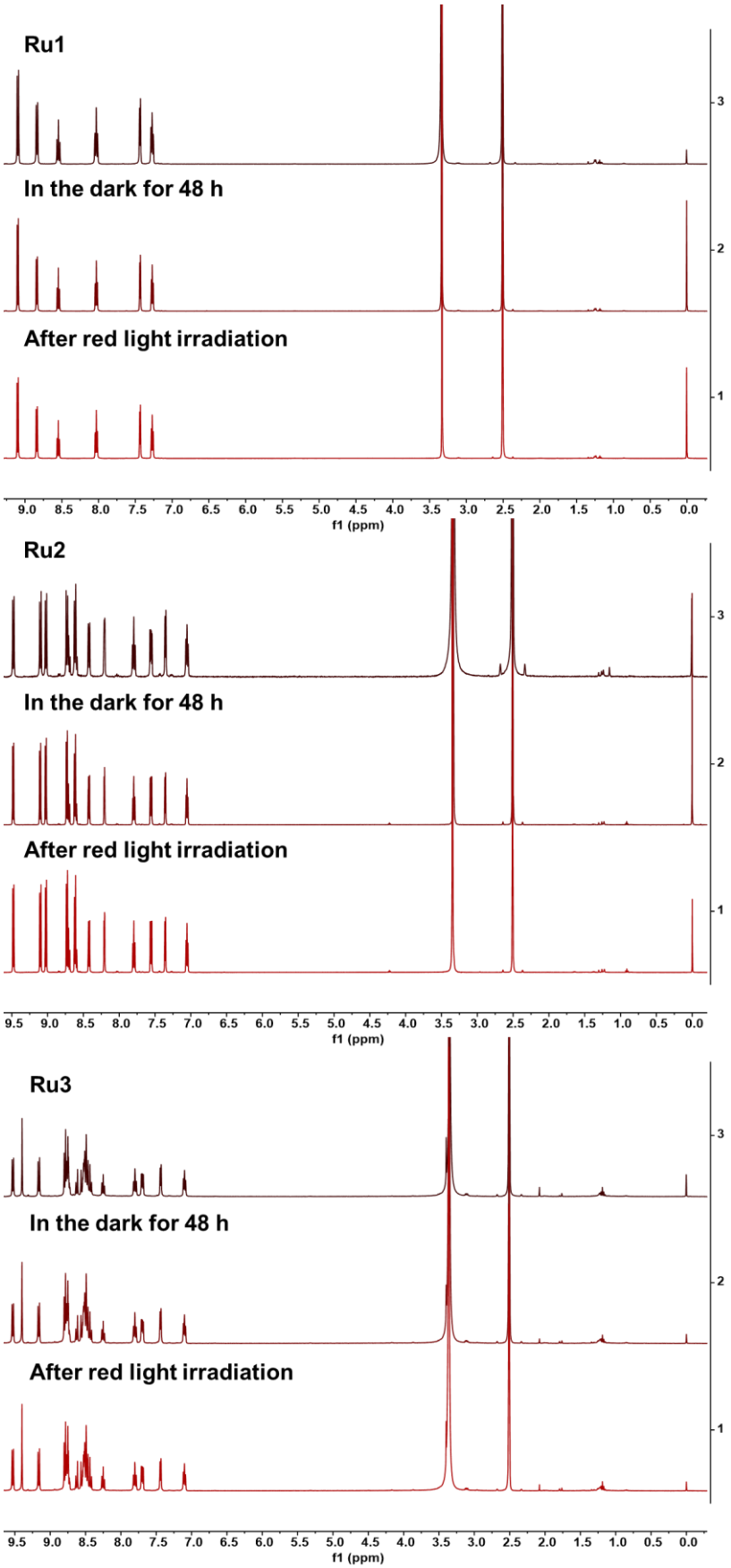

Figure S9. Stability of **Ru1**-**Ru3** determined by ^{1}H NMR in the dark for 48 h or after 635 nm light (63.7 J/cm^{2}).

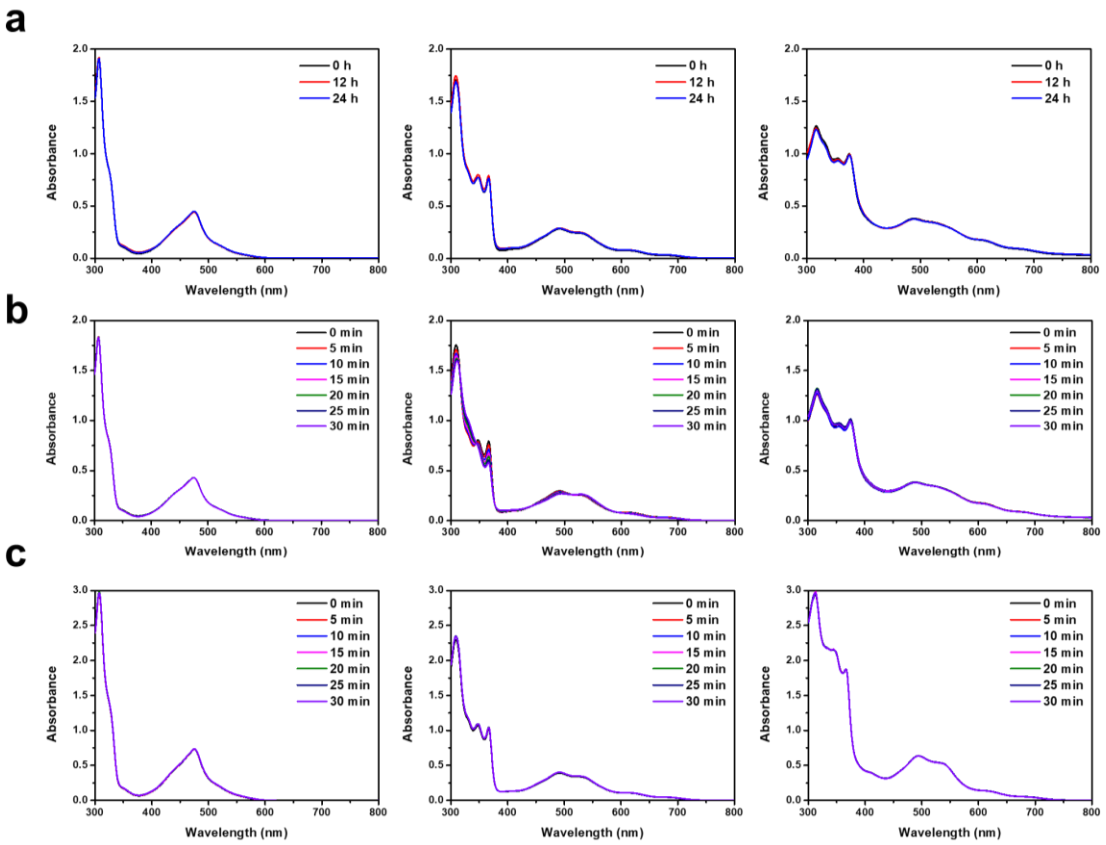

Figure S10. (a) Dark and (b) photo-stability of **Ru1**-**Ru3** in DMEM after 635 nm light (23.59 mW/cm^2). (c) Photo-stability in CH_3CN after 635 nm light (23.59 mW/cm^2).

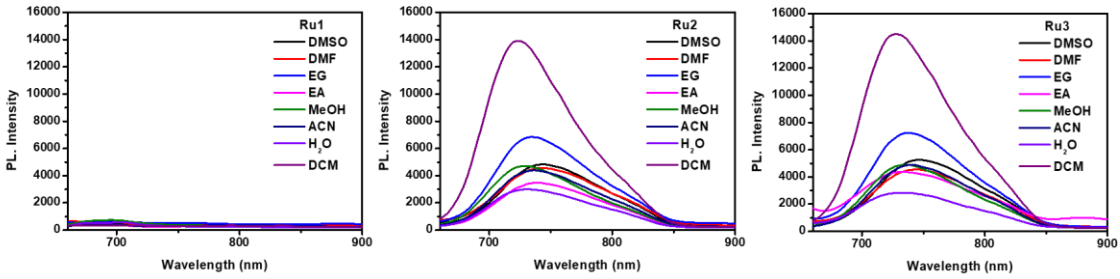

Figure S11. Solvent polarity dependent phosphorescence spectra of **Ru1**-**Ru3** (10 μM) at RT.

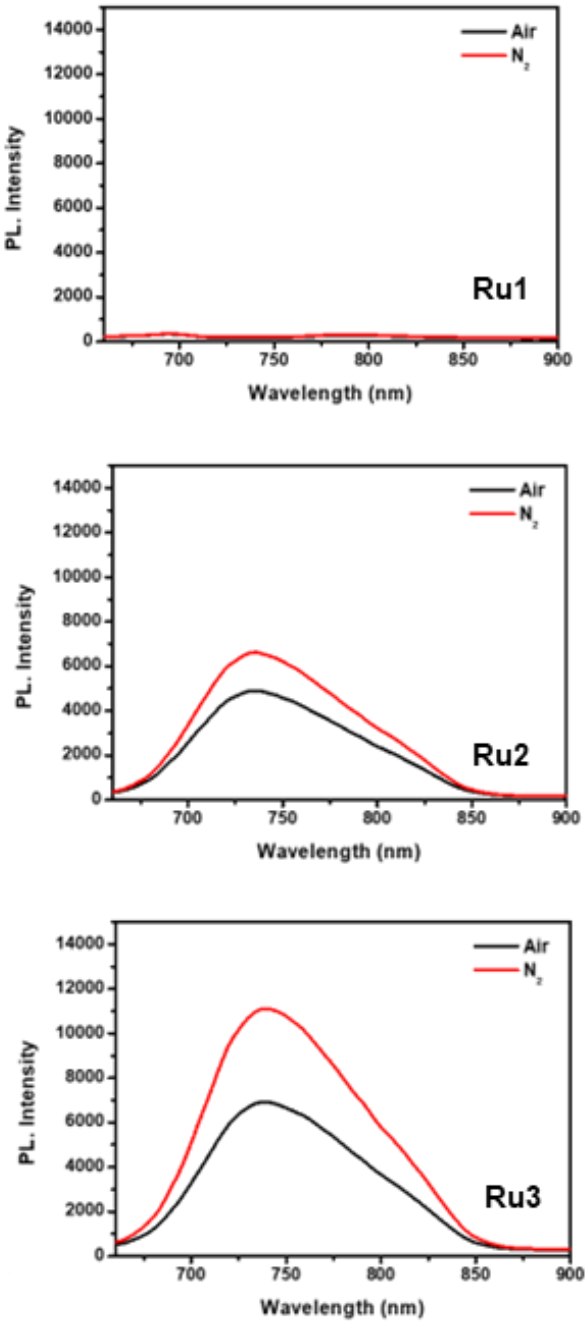

Figure S12. Phosphorescence spectra of **Ru1-Ru3** (10 μM) in air or nitrogen-saturated CH_2Cl_2 at 298 K (λ_{ex} = 635 nm).

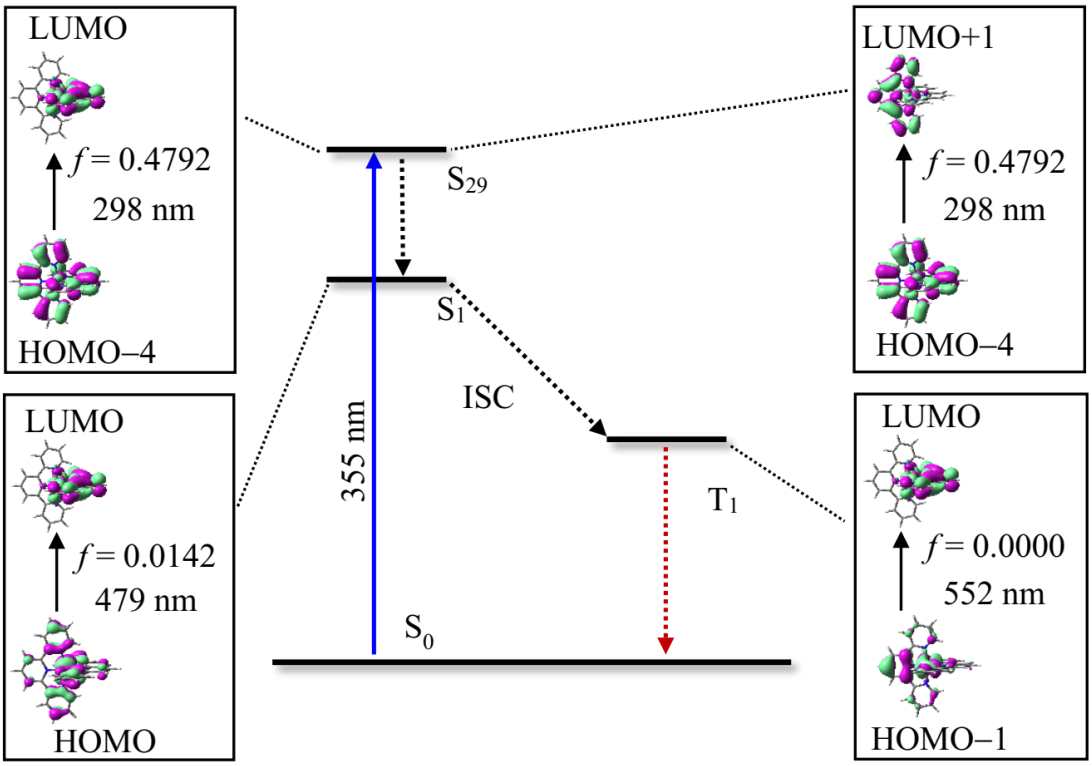

Figure S13. Selected frontier molecular orbitals involved in the singlet and triplet excited states of **Ru1**.The calculations are at the TD-DFT//B3LYP/6-31G(d,p)/SDD /PCM(Acetonitrile) level with Gaussian 16.

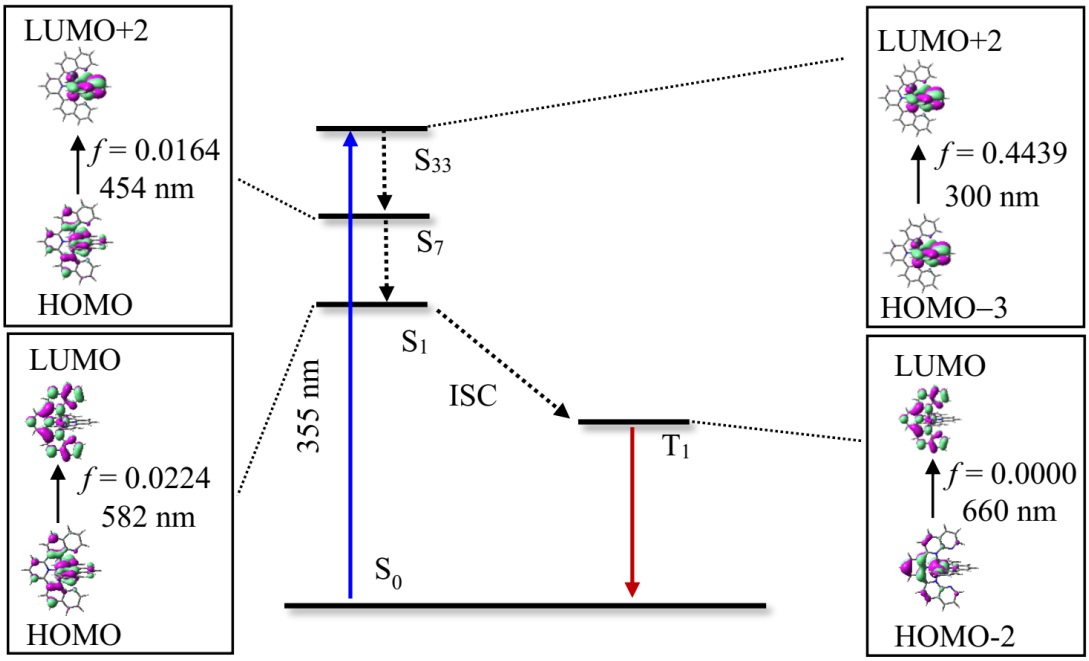

Figure S14. Selected frontier molecular orbitals involved in the singlet and triplet excited states of **Ru2**.The calculations were at the TD-DFT//B3LYP/6-31G(d,p)/SDD /PCM(Acetonitrile) level

with Gaussian 16.

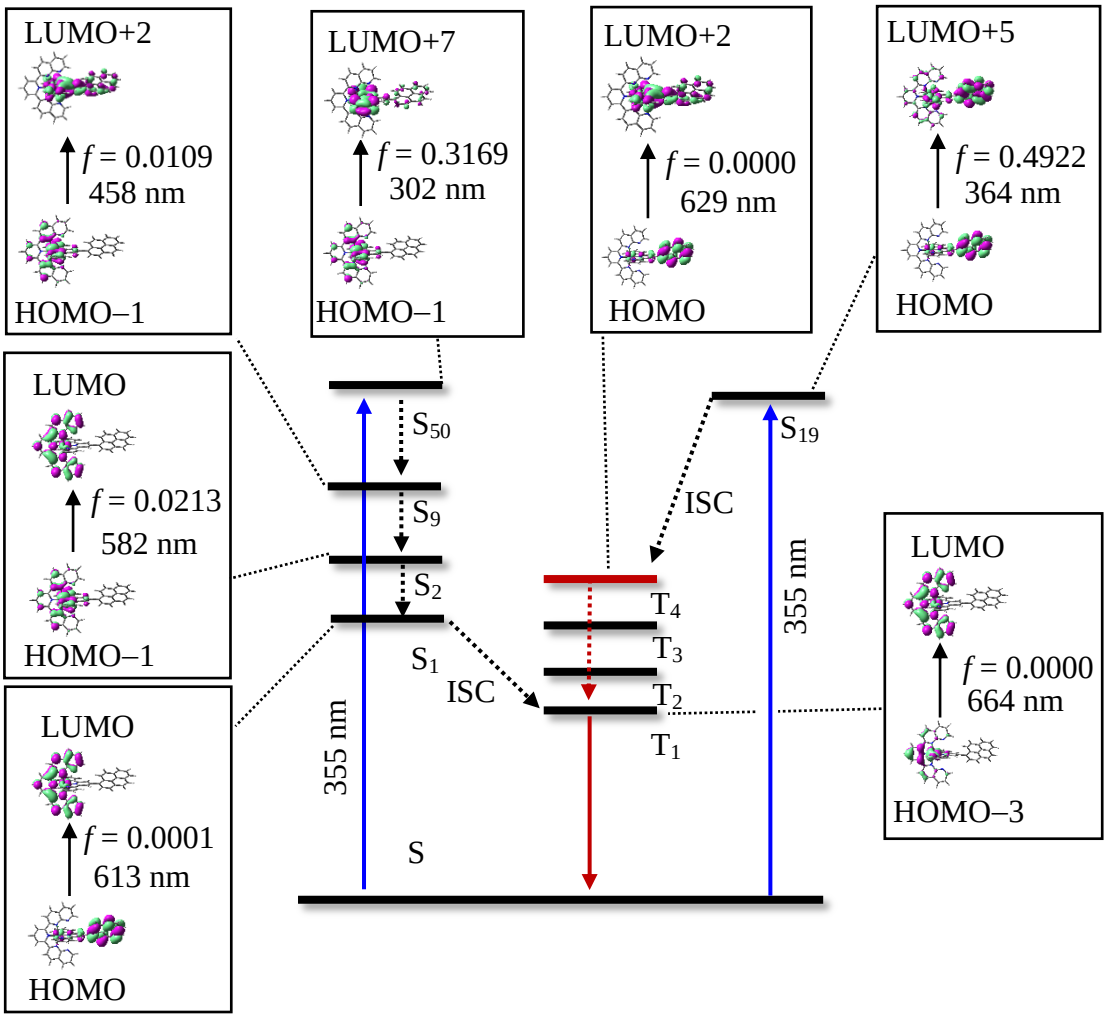

Figure S15. Selected frontier molecular orbitals involved in the singlet and triplet excited states of **Ru3**.The calculations were at the TD-DFT//B3LYP/6-31G(d,p)/SDD /PCM(Acetonitrile) level with Gaussian 16.

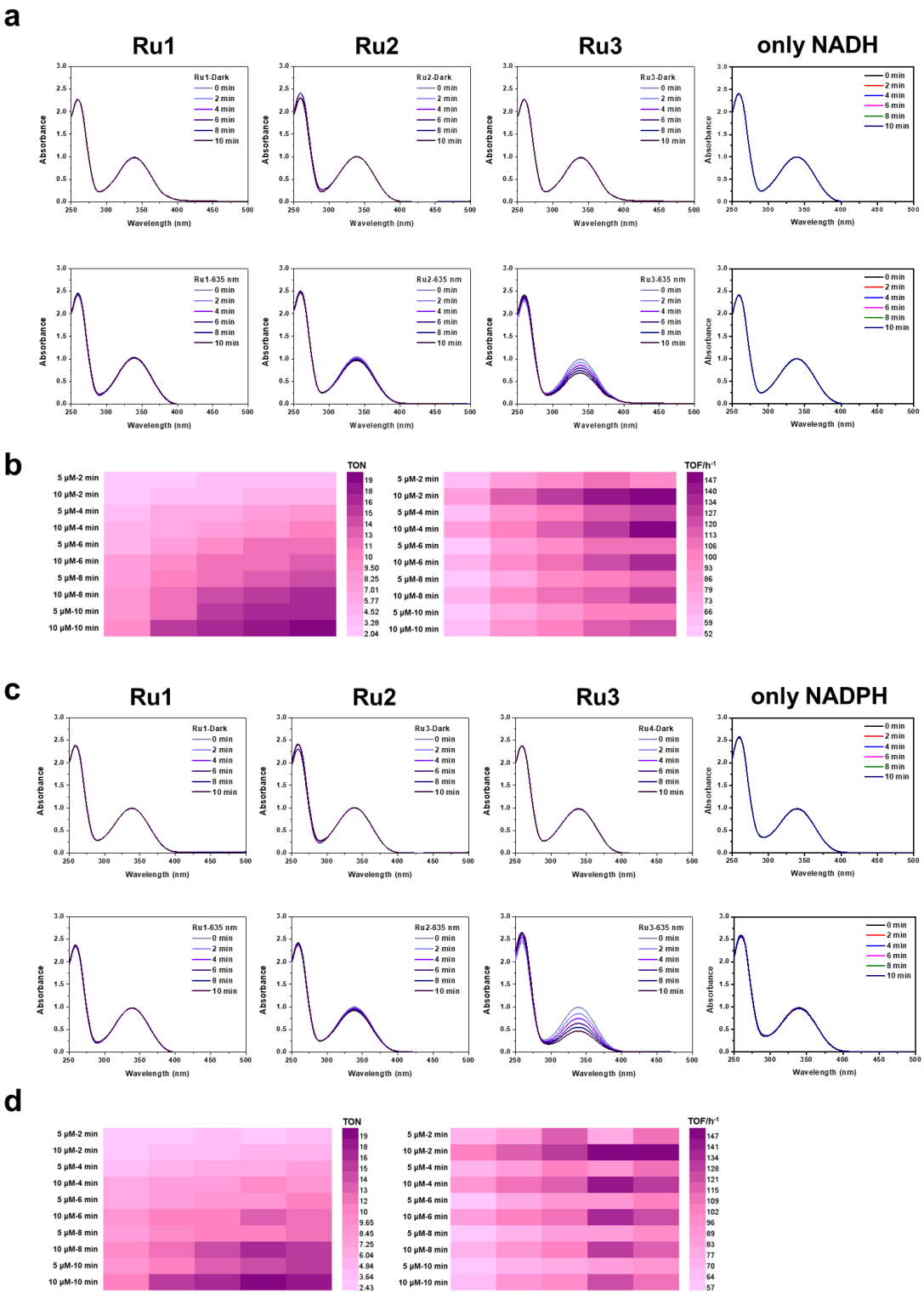

Figure S16. (a) Photocatalytic oxidation of NADH (160 μM) with **Ru1-Ru3** (5 μM) (up) or in the dark (down). (b) TON and TOF of NADH with **Ru3** under irradiation. (c) Photocatalytic oxidation of NADPH (160 μM) with **Ru1-Ru3** (5 μM) (up) or in the dark (down). (d) TON and TOF of NADPH with **Ru3** under red irradiation. Light: 27.08 mW/cm^2, 635 nm.

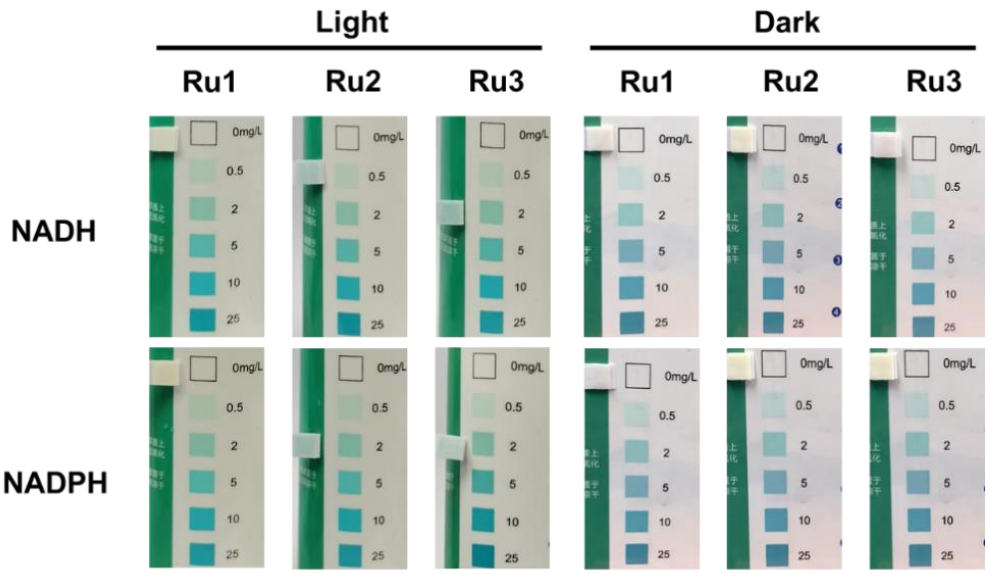

Figure S17. Detection of H_2O_2 generation of **Ru1-Ru3** (50 μM) and NAD(P)H (2.5 mM) after 635 nm light irradiation (42.5 J/cm^2) or in the dark.

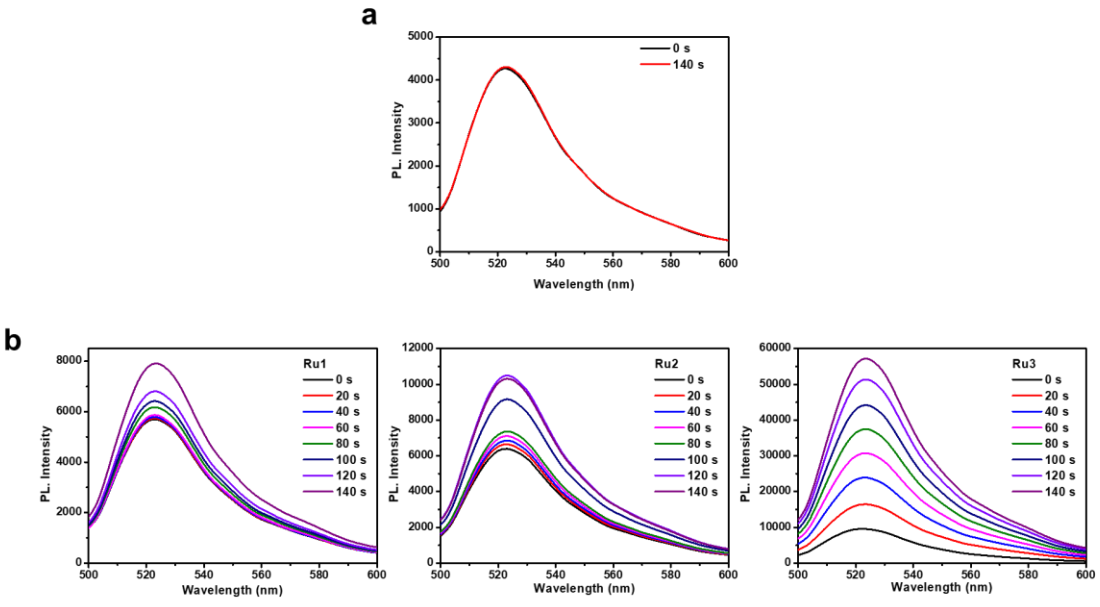

Figure S18. (a) Stability of DHR123 (10 μM) upon 635 nm light irradiation (23.59 mW/cm^2). (b) Detection of superoxide anion generation of **Ru1-Ru3** (5 μM**)** probed by DHR123 (10 μM) after 635 nm light irradiation (23.59 mW/cm^2)**.**

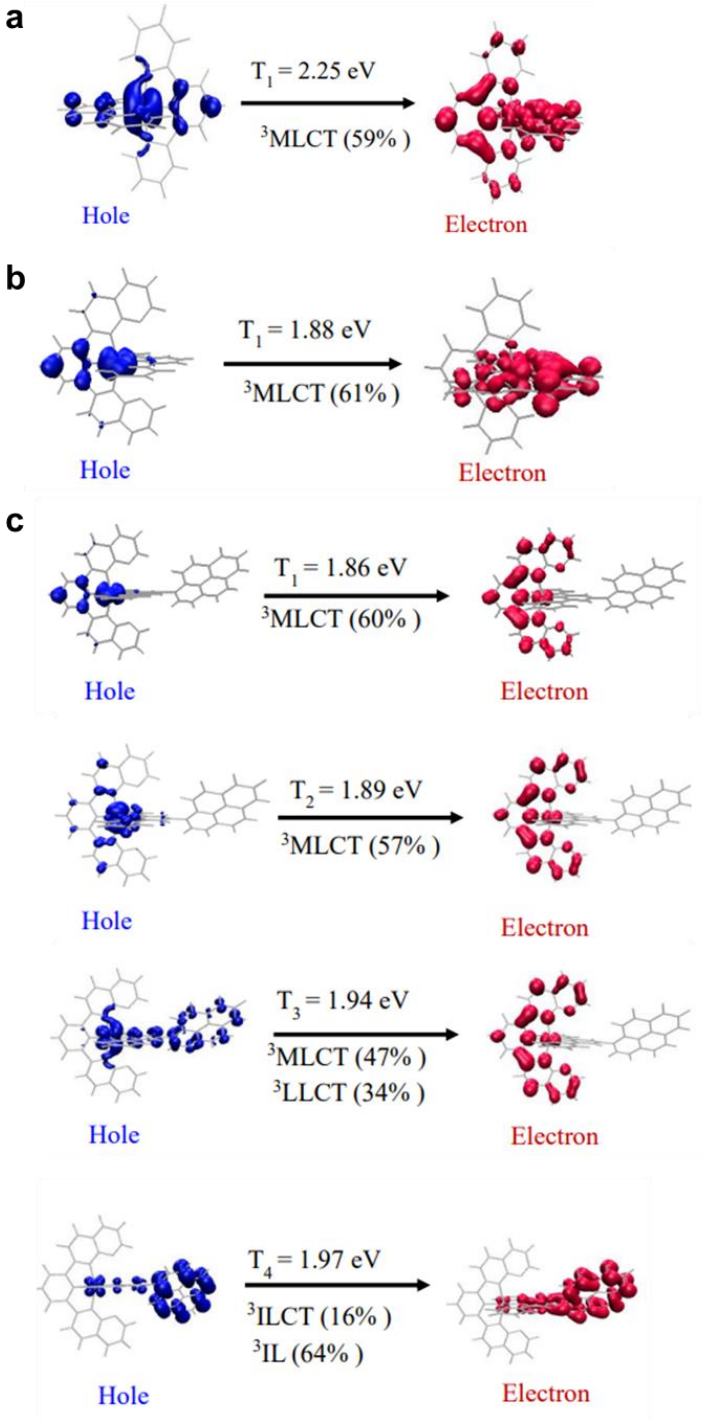

Figure S19. (a) The natural transition orbitals (NTOs) analysis of T_1 state of **Ru1** and the contribution degree to $S_0 \rightarrow T_1$ transition. (b) The natural transition orbitals (NTOs) analysis of T_1 state of **Ru2** and the contribution degree to $S_0 \rightarrow T_1$ transition. (c) The natural transition orbitals (NTOs) analysis of T_n state of **Ru3** and the contribution degree to $S_0 \rightarrow T_n$ transition. Based on the TD-DFT//B3LYP/6-31G(d,p)/SDD /PCM(Acetonitrile) level with Gaussian16.

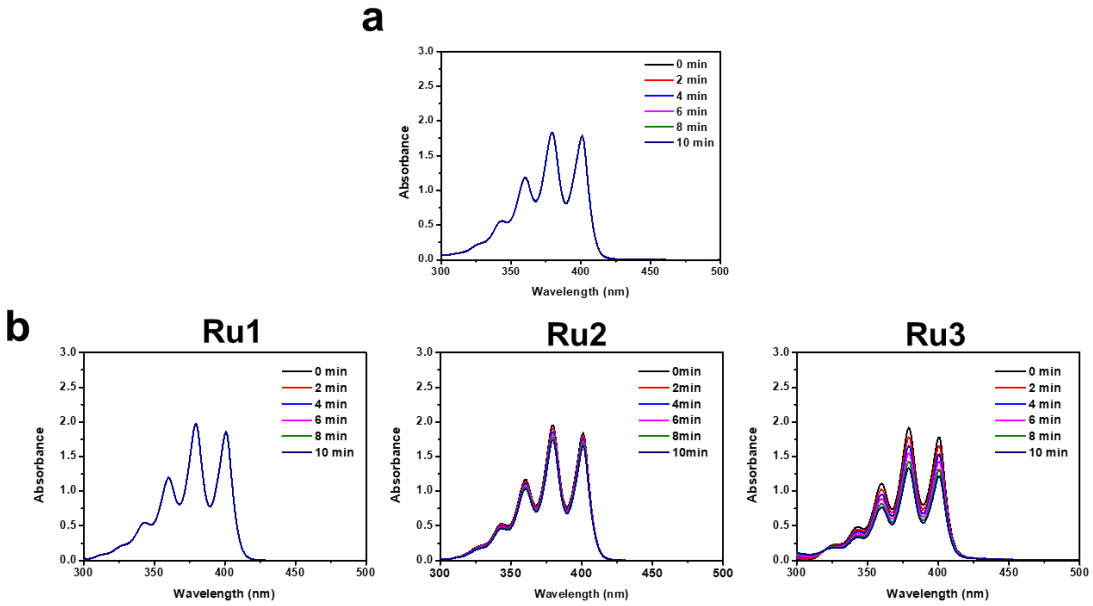

Figure S20. (a) Light-stability of ABDA (200 μM) upon 635 nm light irradiation (27.08 mW/cm^2). (b) $^1O_2$ generation by **Ru1**-**Ru3** (10 μM) in PBS upon irradiation with red light (635 nm, 27.08 mW/cm^2) as was probed by change in absorbance of ABDA (200 μM).

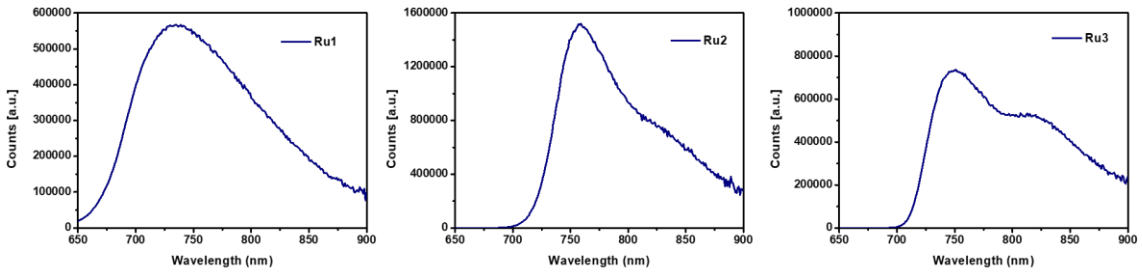

Figure S21. Fluorescence emission spectra of **Ru1**-**Ru3** powders at 77K excited by 635 nm.

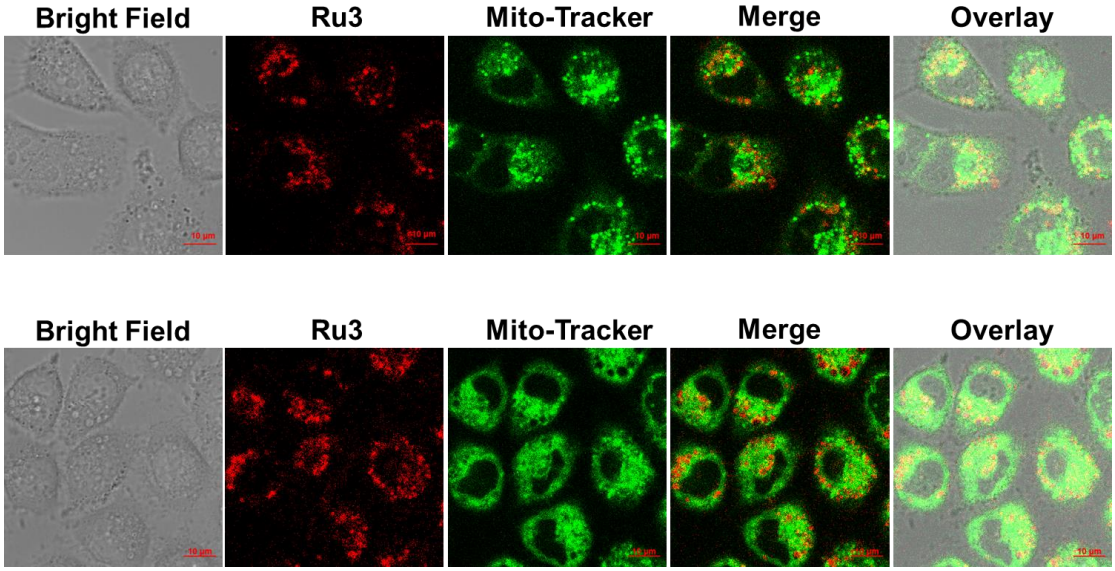

Figure S22. Intracellular localization of **Ru3** in A549/DDP cells. After incubation with **Ru3** (50 μM) for 6 h, A549/DDP cells co-stained with Mito-tracker and Lyso-tracker dyes (100 nM) for 30 min respectively. Scale bar: 10 μm.

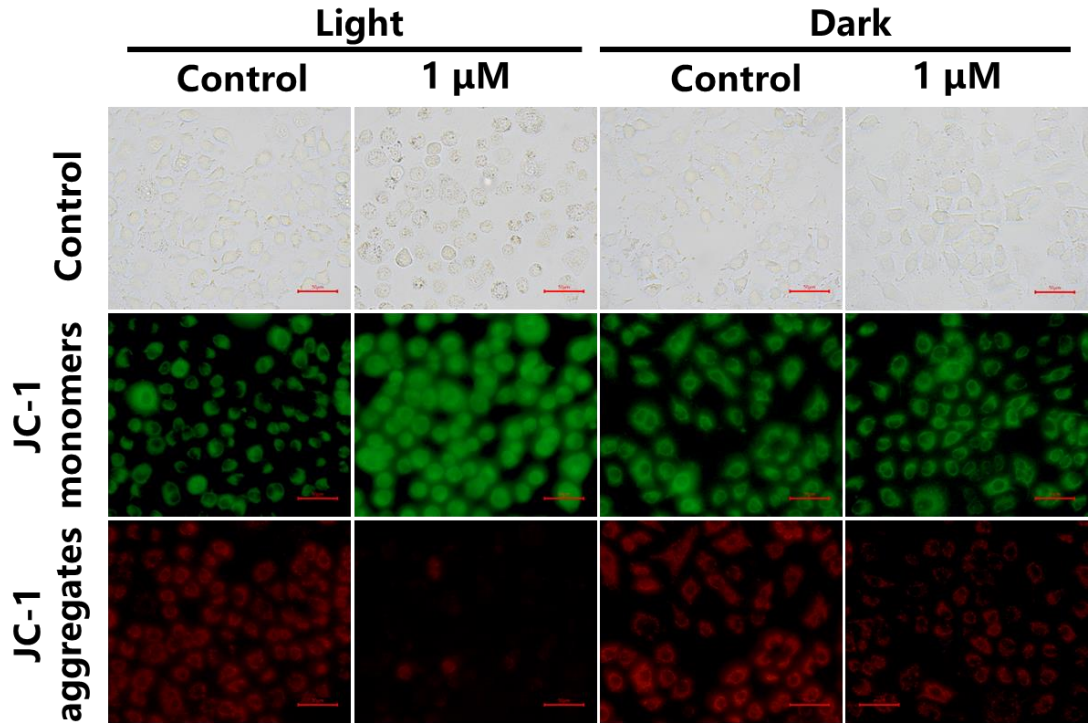

Figure S23. Detection of **Ru3** (1 μM) induced change in the mitochondrial membrane potential of A549/DDP cells after dark or light treatment by JC-1 staining assay, scale bar: 50 μm.

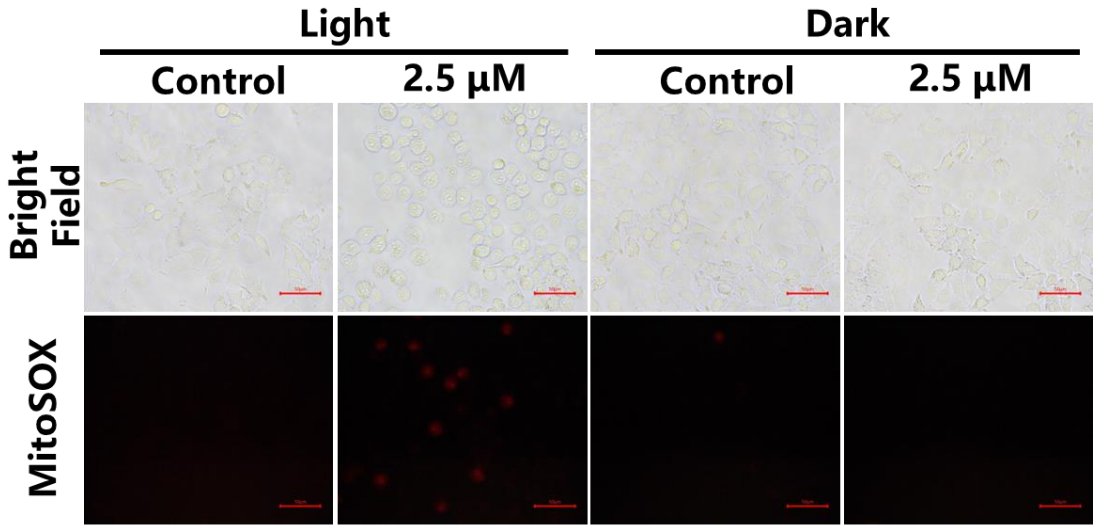

Figure S24. Intracellular mitochondrial superoxide generation by **Ru3** (1 μM), probed by MitoSOX™ Red mitochondrial superoxide indicator (5 μM) with or without red light irradiation (635 nm, 63.7 J/cm^2). Scale bar: 50 μm.

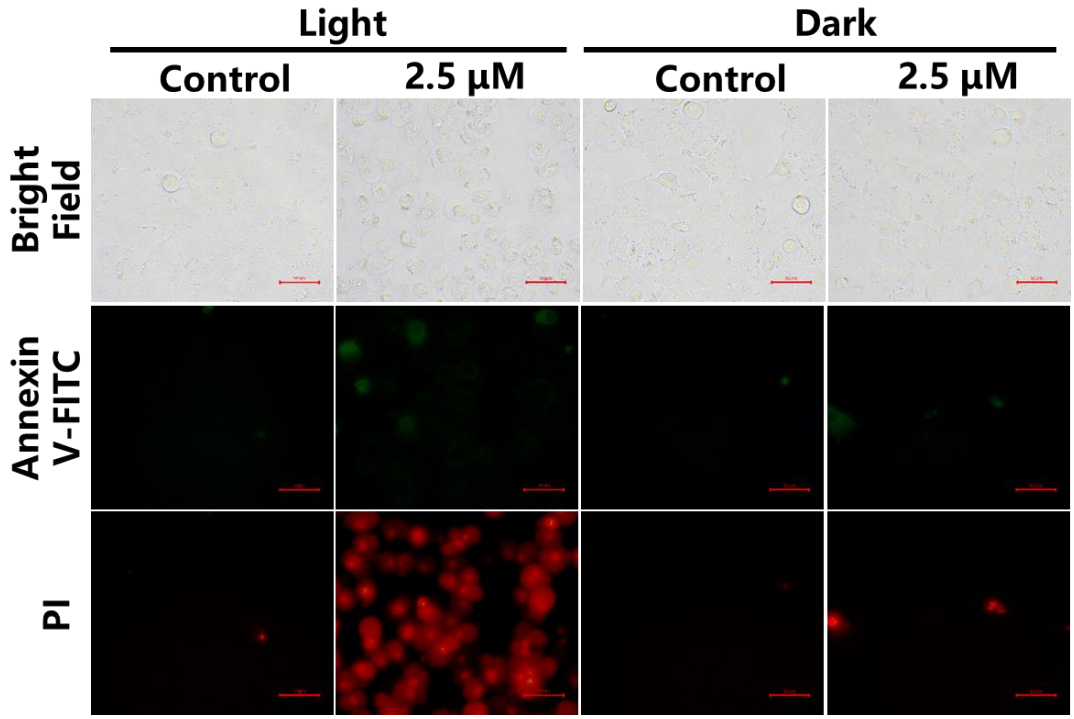

Figure S25. Annexin V-FITC/PI dual staining assay with **Ru3** (2.5 μM) treated A549/DDP cells, scale bar: 50 μm.

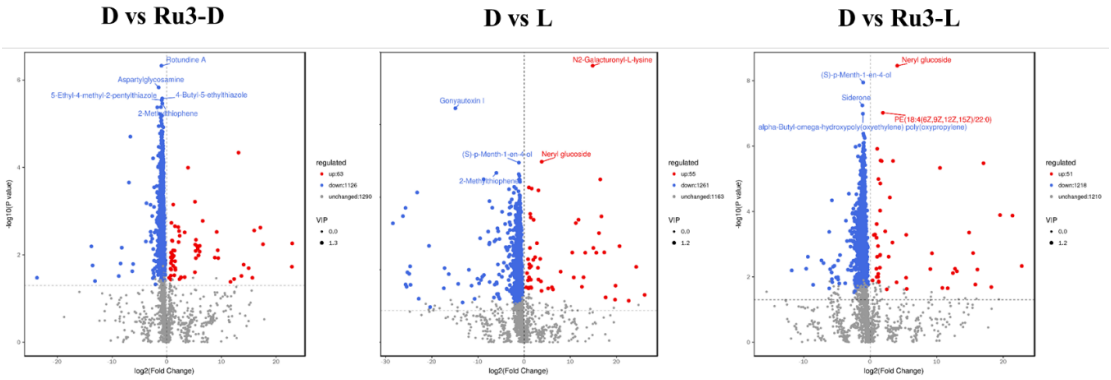

Figure S26. Volcano plot between different groups. Standard: P-value <0.05, VIP > 1, in positive ion mode.

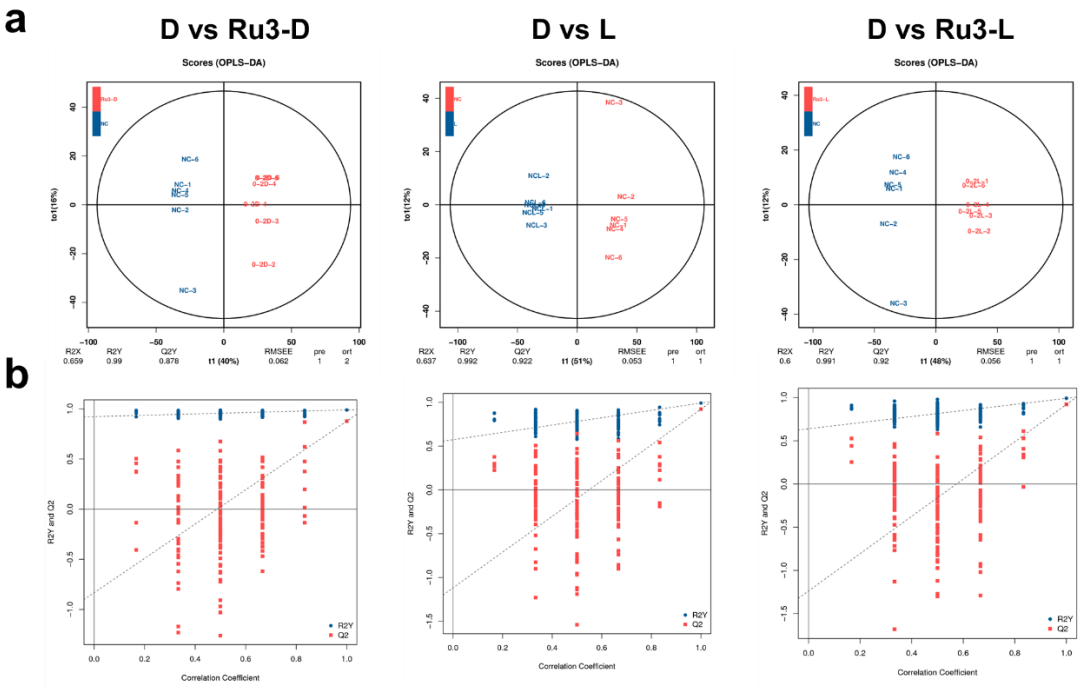

Figure S27. (a) OPLS-DA plots and (b) OPLS-DA scores between different groups, in positive ion mode.

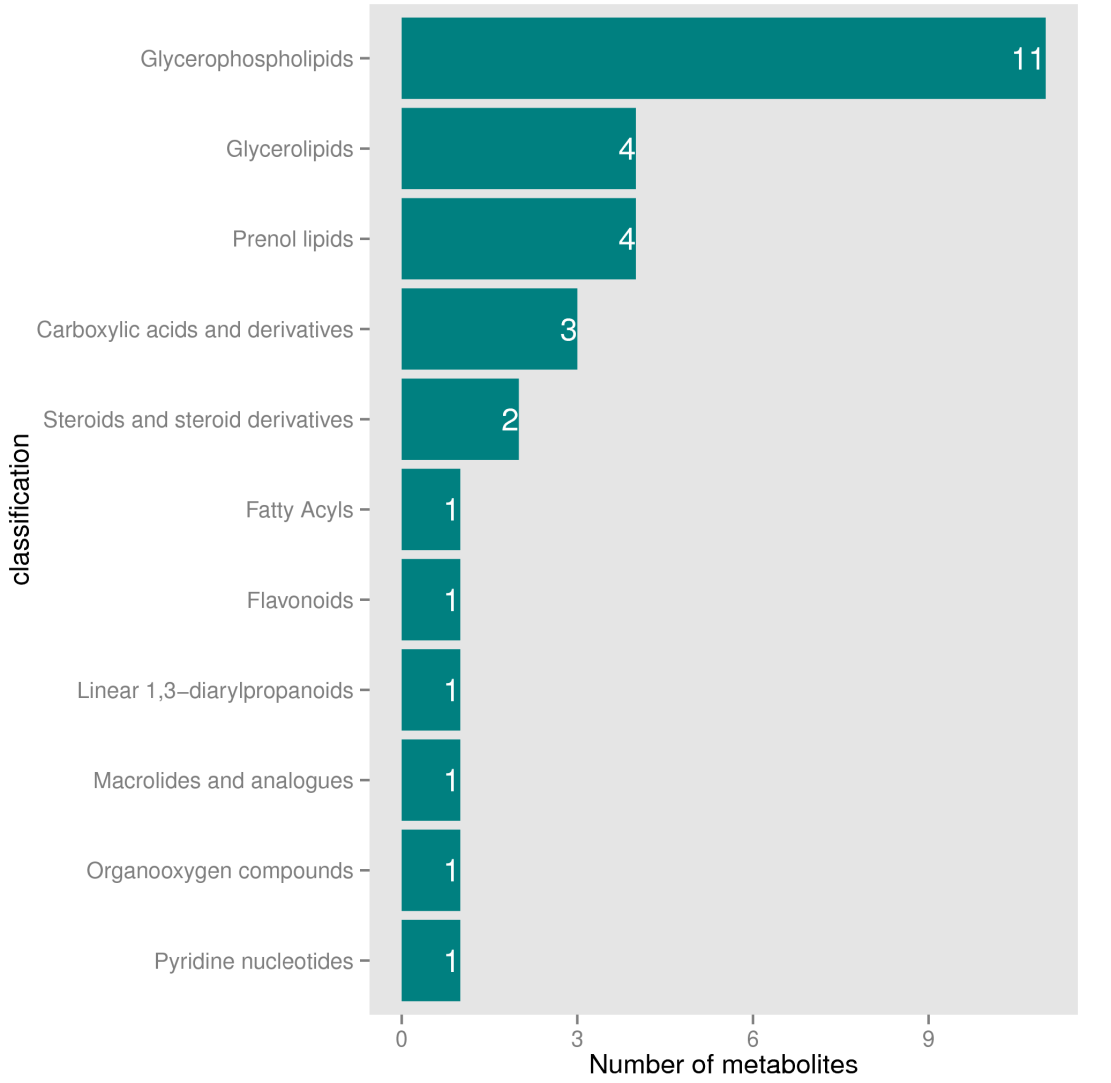

Figure S28. HMDB classification of differential metabolites.

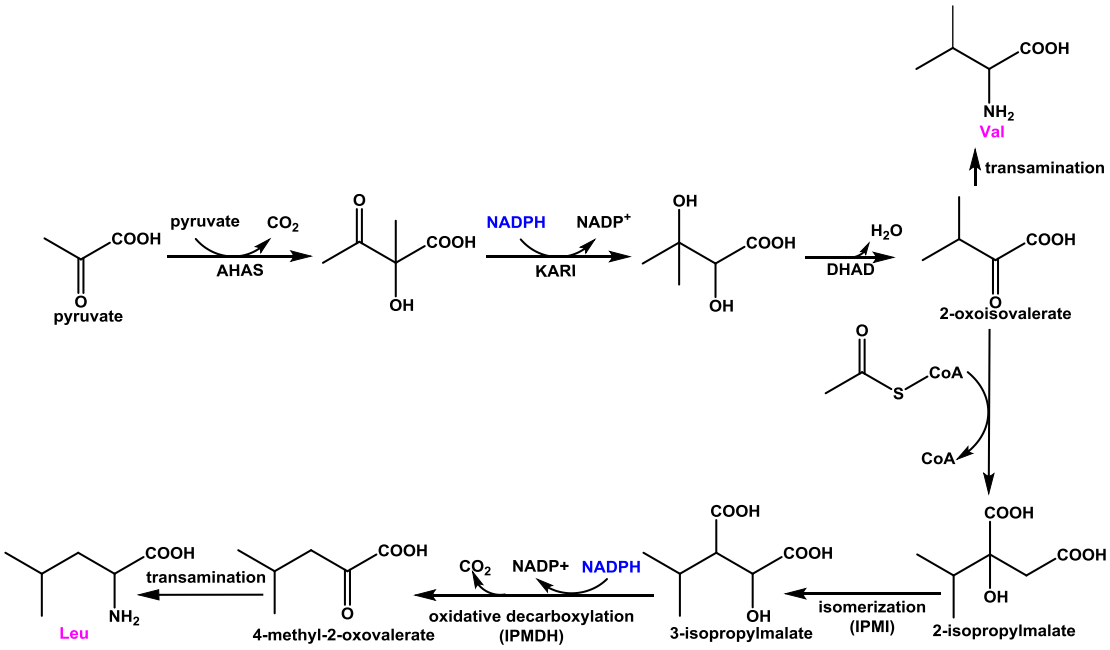

Figure S29. Biosynthetic pathway of Valine (Val) and Leucine (Leu).

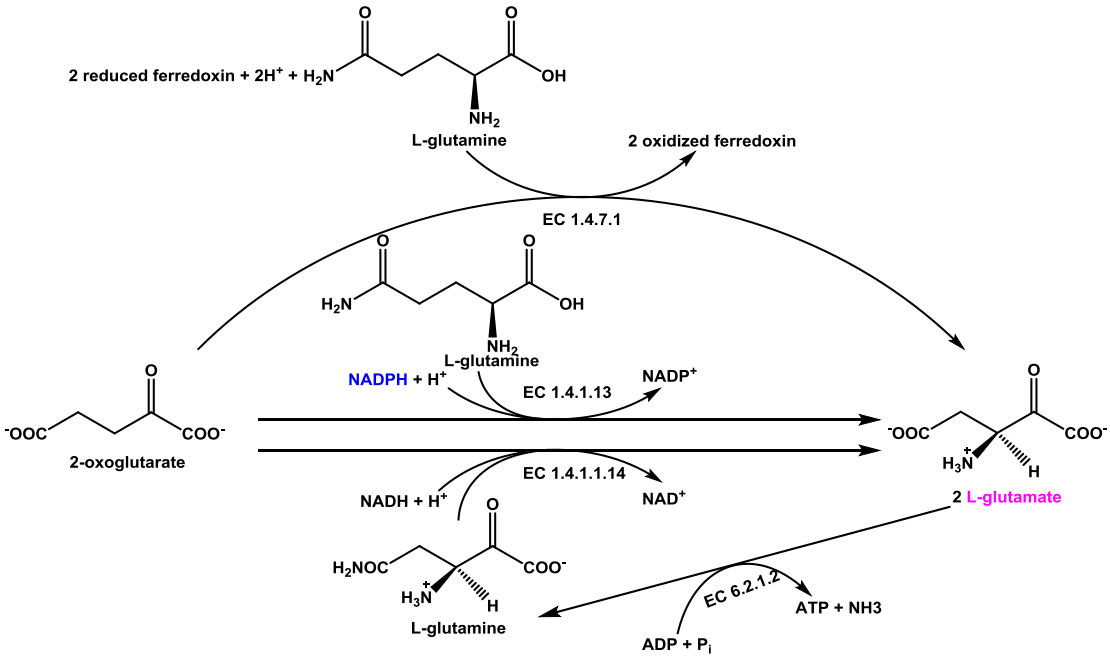

Figure S30. Biosynthetic pathway of L-glutamate.

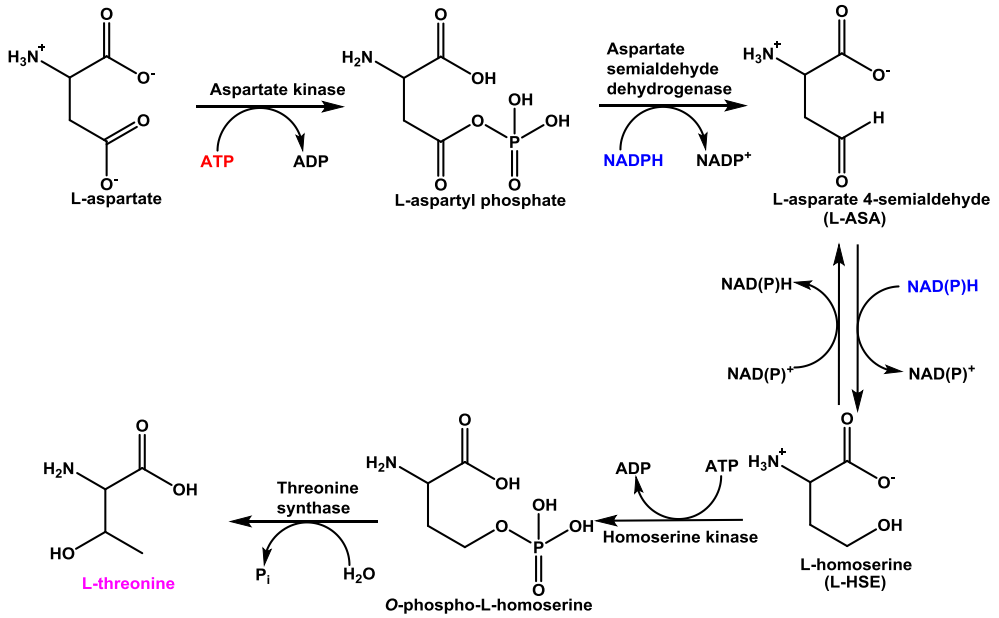

Figure S31. Biosynthetic pathway of L-threonine.

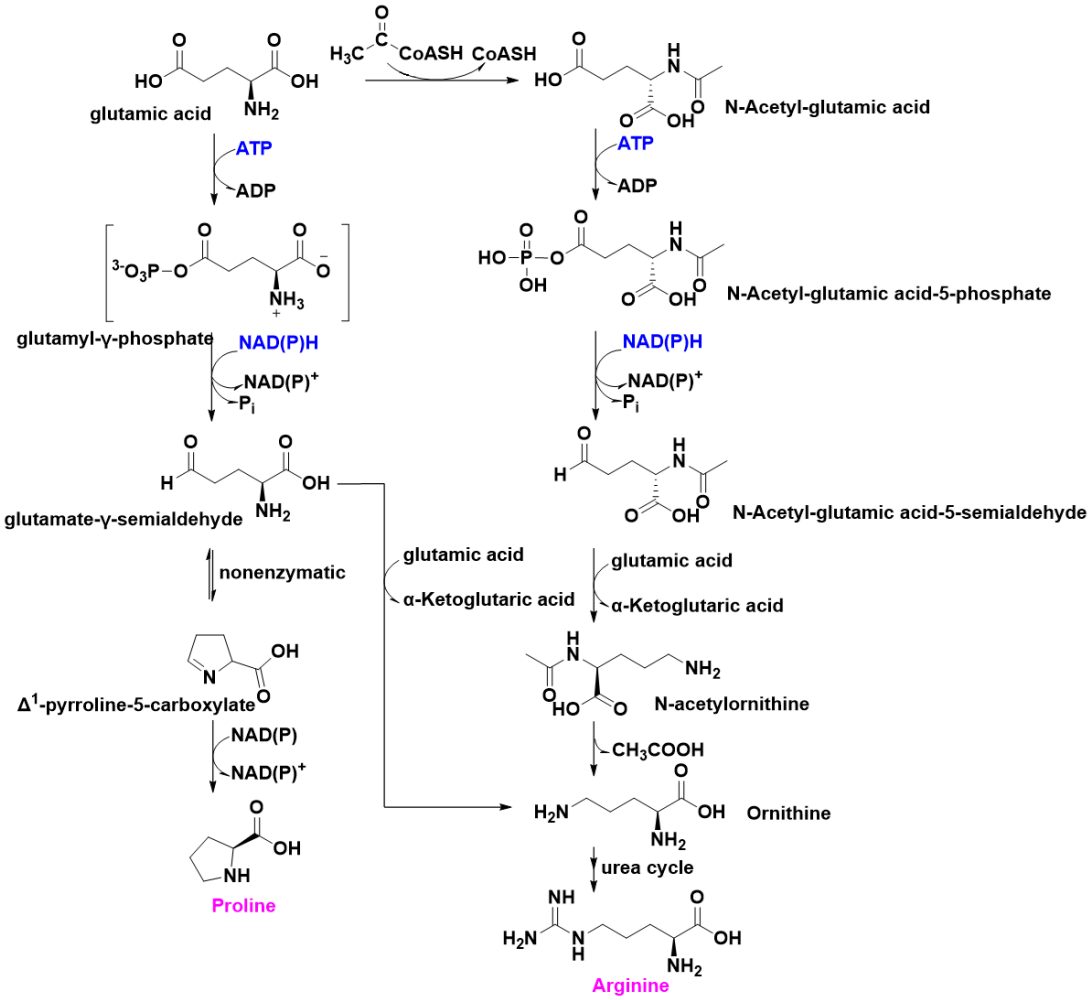

Figure S32. Biosynthetic pathway of Proline and Arginine.

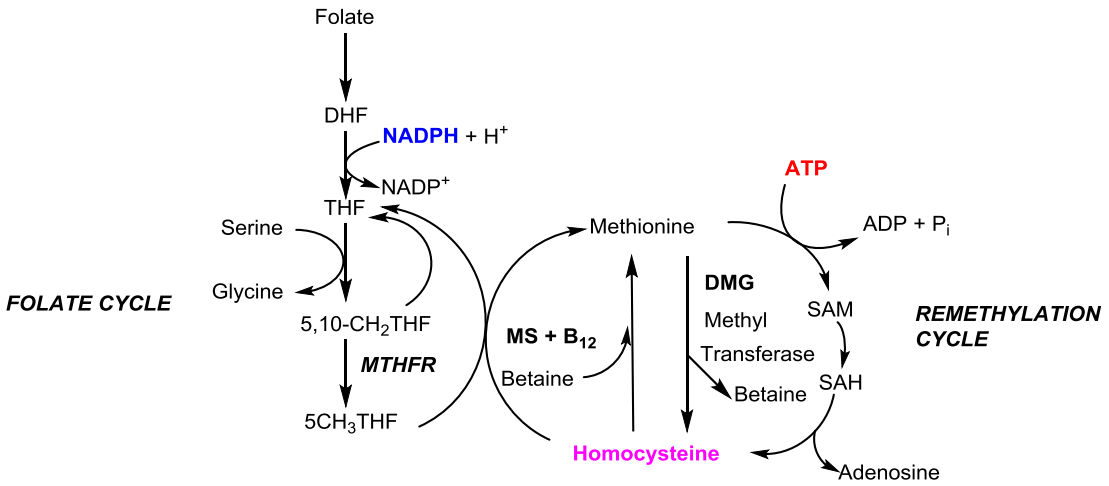

DHF	Deoxyribonucleic Acid	SAM	S-Adenosyl Methionine
THF	Tetrahydrofolate	SAH	S-Adenosyl Homocysteine
MTHFR	Methylene Tetrahydrofolate Reductase	MS	Methionine Synthase
		DMG	Dimethyl Glycine

Figure S33. Homocysteine metabolism and its relation with folate cycle.

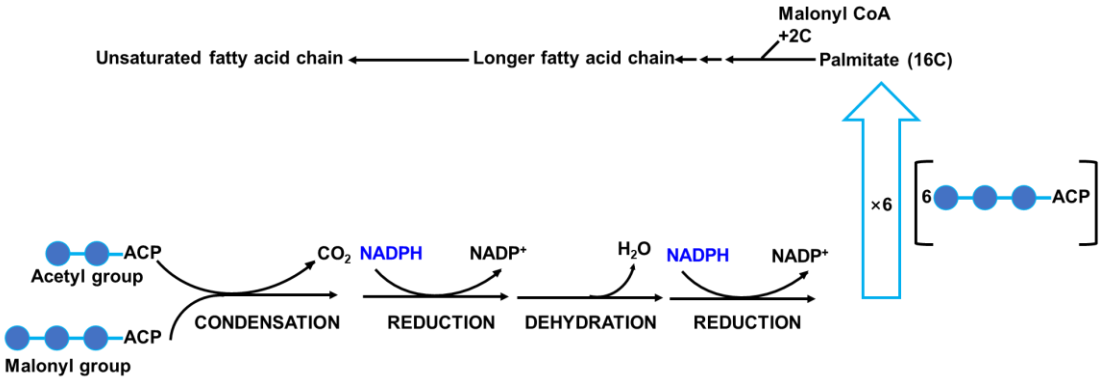

Figure S34. Pathway of fatty acids biosynthesis.

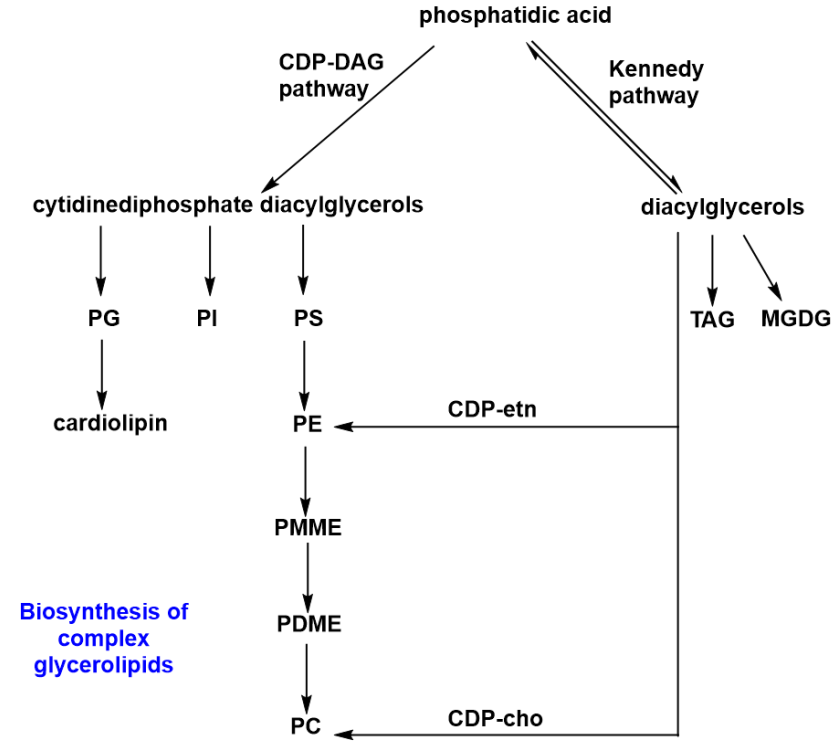

Figure S35. Biosynthesis of complex glycerophospholipids.

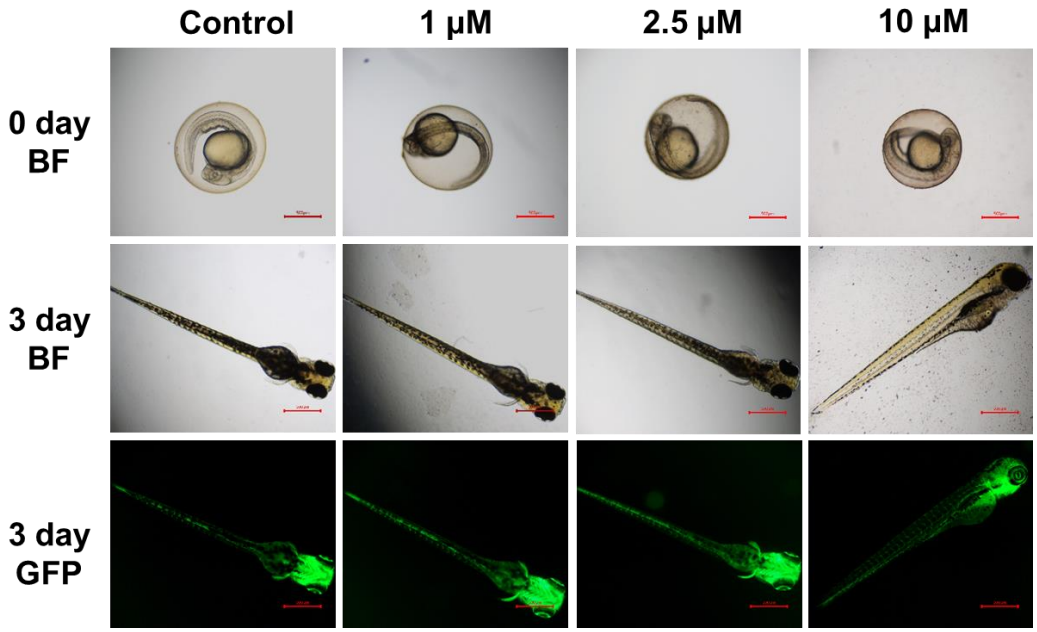

Figure S36. *In vivo* biocompatibility of **Ru3** toward Zebrafish.

Table S1. Photophysical properties of **Ru^{II}** complexes at 298 K.

λ_{abs}[a]/ nm	ε[b]×10^4/ M^{-1}cm^{-1}	λ_{em}[c]/ nm	Φ_p[d]	τ_p/ ns	Φ_Δ[g]

Tables

Table S2. Electrochemical properties of the **Ru^{II}** complexes.

Complex	Ground state[a]				Excited State		
	E_{ox}/V	E_{red}/V			E^*_{red}[c]/V	E^*_{ox}[c]/V	$\Delta E_{\lambda max}$[b]/eV
		I	II	III			
Ru1	+1.27	-1.45	-1.46		n.c.	n.c.	n.c.
Ru2	+1.21	-0.93	-1.18	-1.32	+0.75	-0.47	1.68
Ru3	+1.21	-0.93	-1.20	-1.29	+0.75	-0.47	1.68

[a] All complexes were measured in 0.1 M Bu_4NPF_6–CH_3CN; *T* = 25 ℃; scan rate = 100 mV/s. $E_{1/2}$ (Fc^+/Fc) was set as 0 V in the cyclic voltammograms. E_{ox} (vs SCE) = 0.38 + E_{ox} (vs Ferrocene) and E_{red} (vs SCE) = 0.38 + E_{red} (vs Ferrocene).

[b] $\Delta E_{\lambda max}$ ($\Delta E_{\lambda max}$ = 1240/λ), λ is the wavelength of emission maximum in fluorescence emission spectra.

[c] The corresponding oxidation and reduction potentials in the excited state (vs SCE) are estimated from the oxidation/reduction potentials in the ground state and the energy of the emission maximum in CH_3CN. E^*_{ox} = E_{ox} - $\Delta E_{\lambda max}$; E^*_{red} = E_{red}(I) + E_{00} ≈ E_{red}(I) + $\Delta E_{\lambda max}$; M represents metal complex or photocatalyst.

n.c. = not calculated.

Ru1	476	2.04/0.01	567/728	n.d.	n.d.	n.d.
Ru2	530	0.98/0.29	736	0.0024/0.0004	159.24[e]/176.59[f]	0.08
Ru3	495	1.52/0.24	740	0.0022/0.0001	189.71[e]/252.11[f]	0.19

[a] Absorbance maximum wavelength in CH_2Cl_2 (1×10^{-5} M). [b] Molar absorption coefficient at absorbance maximum wavelength and 635 nm. [c] λ_{ex} = 635 nm, in CH_2Cl_2 (1×10^{-5} M). [d] Phosphorescence quantum yields, used MB in CH_3CN or water as the reference. [e] Measured in aerated CH_3CN, fitted with monoexponential equation. [f] Measured in deaerated CH_3CN, fitted with monoexponential equation. n.d. = not determined. [g] Φ_Δ refers to the $^1O_2$ generation quantum yield with the standard MB (Φ_Δ = 0.52 in aqueous solution).

Table S3. Main electronic transition, electronic excitation energies (eV), corresponding oscillator strengths (*f*), CI coefficients and excited state character of **Ru1**-**Ru3**, all data were collected below, and calculated by TD-DFT//B3LYP/6-31G(d,p)/SDD/PCM (Acetonitrile) level, based on the DFT//PBE0/6-31G(d,p)/SDD-optimized ground state.

	Electronic Transition	Energy (eV/nm)	*f*	Composition	CI	Character
Ru1	$S_0 \rightarrow S_1$	2.59/479	0.0142	H→L	0.8712	MLCT
	$S_0 \rightarrow S_7$	2.99/415	0.1672	H→L+2	0.7333	MLCT
	$S_0 \rightarrow S_{29}$	4.15/298	0.4792	H–4→ L	0.3362	IL
				H–4→ L+1	0.3042	IL
	$S_0 \rightarrow T_1$	2.25/552	0.0000	H–1→L	0.4050	MLCT
Ru2	$S_0 \rightarrow S_1$	2.13/582	0.0224	H→L	0.9688	MLCT
	$S_0 \rightarrow S_7$	2.73/454	0.1672	H→L+2	0.9522	MLCT
	$S_0 \rightarrow S_{33}$	4.13/300	0.4439	H–3→L+2	0.6265	IL
	$S_0 \rightarrow T_1$	1.88/660	0.0000	H–2→L	0.9357	MLCT
Ru3	$S_0 \rightarrow S_1$	2.02/613	0.0001	H→L	0.6227	LLCT
				H–2→L	0.3528	MLCT
	$S_0 \rightarrow S_2$	2.13/582	0.0213	H–1→L	0.7040	MLCT
	$S_0 \rightarrow S_4$	2.39/517	0.0132	H–3→L	0.5060	MLCT
				H–1→ L+1	0.3698	LLCT
	$S_0 \rightarrow S_9$	2.70/458	0.0109	H–1→ L+2	0.7938	MLCT
	$S_0 \rightarrow S_{19}$	3.40/364	0.4922	H→L+5	0.7843	IL/ILCT
	$S_0 \rightarrow S_{50}$	4.09/302	0.3169	H–1→L+7	0.4268	IL
				H–5→L+2	0.4544	MLCT
	$S_0 \rightarrow T_1$	1.87/664	0.0000	H–3→L	0.9056	MLCT
	$S_0 \rightarrow T_2$	1.89/657	0.0000	H–1→L	0.9248	MLCT
	$S_0 \rightarrow T_3$	1.94/638	0.0000	H–2→L	0.4518	MLCT
	$S_0 \rightarrow T_4$	1.97/629	0.0000	H→ L+2	0.4418	IL/ILCT

Table S5. Terpyridine-based Ru(II) photosensitizers reported in previous work.

Table S4. Dark IC_{50} values (μM) of **Ru1-Ru3** toward non-tumorigenic cell lines and A549.

Cell line	IC_{50}	Ru1	Ru2	Ru3
NCM460	Dark[a]	>100	>100	>100
HUEVC	Dark[a]	>100	>100	>100
HDFa	Dark[a]	>100	>100	>100
A549	Dark[a]	>100	>100	>100
	Light[b]	>100	$7.7^{\pm 0.2}$	$0.09^{\pm 0.01}$
	PI[c]	n.a.	12.9	1111.11

[a] 4 h drug exposure in the dark, replaced with fresh medium followed by 44 h incubation.

[b] 4 h drug exposure in the dark, replaced with fresh medium and red-light irradiation (635 nm, 63.7 J/cm^2) followed by 44 h incubation.

[c] PI = IC_{50}(Dark) / IC_{50}(Light).

Complex	Cell Line	Light source/nm	IC_{50}(Light) /μM	IC_{50}(Dark) /μM	PI	Ref.
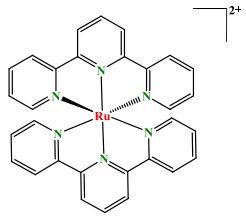	HL60	405 450	~50 ~50	~65	~1.3 ~1.3	[13]
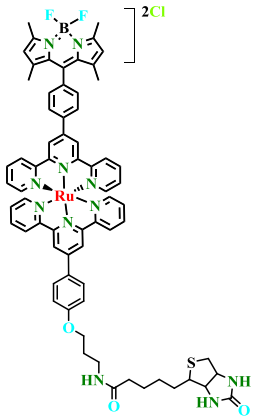	A549	400- 700	0.16 ±0.01	>100	>625	[14]
	HeLa	400- 700	0.07 ±0.01	>100	>1428	
	HPL1D	400- 700	0.54 ±0.04	>100	>185	
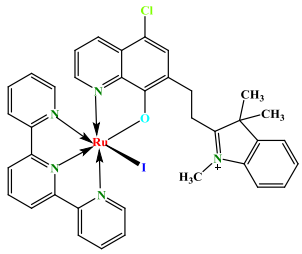	MCF-7	660	3.1	43	13.9	[15]
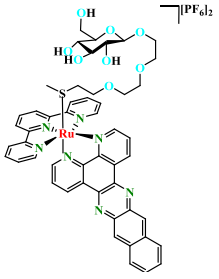	A549	454	0.72 ±0.16	19 ±4.0	26	[16]
	MCF-7	454	0.86 ±0.21	9.6 ±2.9	11	
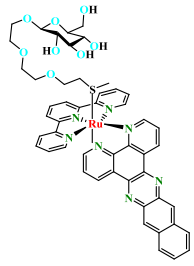	A549	454	0.58 ±0.13	50 ±17	86	[16]
	MCF-7	454	0.61 ±0.28	18 ±3.8	30	

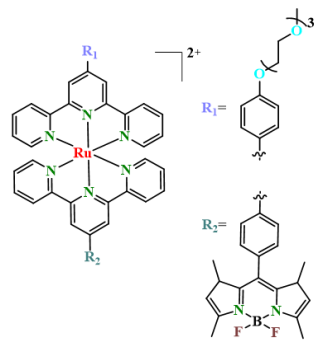	A549	500	1.5	53	35.3	[17]
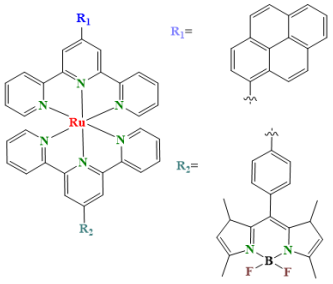	A549	500	11.1	36.3	3.27	[17]
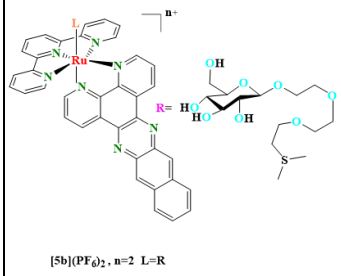 [5b](PF$_6$)$_2$, n=2 L=R	A549	454 ± 11	0.72 ± 0.16	18.72	26	[18]
	MCF-7	454 ± 11	0.86 ± 0.21	9.46	11	
Ru3	A549	635	0.09 ± 0.1	>100	1111	This work
	A549/DDP	635	0.12 ± 0.1	>100	833	

Table S6. Significant differential metabolites detected in D vs **Ru3**-L group compared with D vs L and D vs **Ru3**-D group upon positive ion (filter criteria: FC>1, p value<0.05 and VIP>1).

Name of metabolites	**P value**	**log_2FC**	**VIP**	**Regulation**
DG(18:0/20:4(8Z,11Z,14Z,17Z)/0:0)	0.000003	3.43	1.40	up
Isovitexin 2"-(6"'-p-coumaroylglucoside)	0.000010	1.24	1.33	up
Humulol	0.000123	-0.81	1.31	down
6,10,14-Trimethyl-2-methylenepentadecanal	0.000129	19.54	1.35	up
DG(18:1n7/0:0/18:2n6)	0.000133	21.39	1.36	up
Yucalexin B5	0.000241	0.98	1.24	up
Kanokoside A	0.000244	-1.85	1.30	down
N,N'-Diacetylchitobiosyldiphosphodolichol	0.000451	-1.76	1.26	down
Portensterol	0.000504	0.73	1.21	up
DG(18:0/22:5(4Z,7Z,10Z,13Z,16Z)/0:0)	0.000516	5.42	1.30	up
PC(18:3(9Z,12Z,15Z)/22:1(13Z))	0.000523	0.57	1.18	up
PE(14:0/24:0)	0.000635	0.97	1.23	up
PE(22:5(7Z,10Z,13Z,16Z,19Z)/P-18:1(11Z))	0.000662	-0.69	1.25	down
3-Acetoxyscirpene-4,15-diol	0.001140	1.18	1.17	up
PC(14:0/0:0)	0.001209	-0.87	1.16	down
LysoPC(20:3(8Z,11Z,14Z))	0.001405	-1.01	1.16	down
Netilmicin	0.001582	-0.68	1.22	down
5,8,11-Eicosatriynoic Acid	0.001900	9.29	1.15	up
PG(18:0/18:1(11Z))	0.001992	-0.80	1.19	down
4'-Methoxychalcone	0.002023	-1.19	1.16	down

Ile Gln	0.003179	-2.50	1.15	down
PS(16:1(9Z)/18:0)	0.003470	-0.78	1.18	down
PA(16:0/18:2(9Z,12Z))	0.004229	-0.74	1.14	down
PE(17:0/0:0)	0.004341	-0.88	1.12	down
3-Decaprenyl-4,5-dihydroxybenzoate	0.004514	-0.64	1.14	down
LysoPC(20:4(5Z,8Z,11Z,14Z))	0.004714	-0.87	1.10	down
Estriol	0.005423	-0.54	1.16	down
N-lactoyl-Methionine	0.005826	-1.52	1.07	down
all-trans-3,4-Didehydroretinoate	0.005841	-1.25	1.08	down
3-Hexylpyridine	0.005957	-0.79	1.03	down
9,12-Octadecadiynoic Acid	0.006041	-0.57	1.06	down
Nicotinamide ribotide	0.006074	-1.09	1.07	down
23-Acetoxysoladulcidine	0.006156	-0.96	1.11	down
SM(d18:0/20:2(11Z,14Z))	0.006436	-0.65	1.10	down
DG(20:4(8Z,11Z,14Z,17Z)/18:0/0:0)	0.006793	-1.06	1.12	down
2,5-Octadien-1-ol	0.006871	-1.23	1.08	down
6-[5]-ladderane-1-hexanol	0.007702	-0.95	1.03	down
alpha-Zearalenol	0.007734	-1.73	1.11	down
Levonorgestrel	0.007959	-0.98	1.03	down
Glycerol 2-(9Z,12Z-octadecadienoate) 1-hexadecanoate 3-O-[alpha-D-galactopyranosyl-(1->6)-beta-D-galactopyranoside]	0.008310	-0.76	1.11	down
Homocysteine	0.00849	-1.21	1.0	down

	3		2	
3-Hydroxymugineic acid	0.008762	-1.55	1.06	down
Glu Arg	0.008965	-1.53	1.08	down
RG-108	0.009253	-1.70	1.12	down
PE(DiMe(13,5)/MonoMe(11,3))	0.009567	-0.44	1.08	down
Norbixin	0.009770	-0.98	1.11	down
Scorzoside	0.010167	-1.49	1.06	down
7a,12a-Dihydroxy-cholestene-3-one	0.010214	-4.85	1.10	down
Cycloalliin	0.010410	-5.12	1.06	down
Pitavastatin	0.010571	-0.84	1.02	down
Phytol	0.010575	-0.60	1.09	down
Capecitabine	0.011634	-1.02	1.01	down
3-Hydroxychavicol 1-glucoside	0.011944	-4.81	1.02	down
Ile Val	0.012073	-2.11	1.06	down
Nonoxynol-9	0.012393	-0.86	1.04	down
Inosine	0.012450	-1.26	1.01	down
Quinquenoside L1	0.012819	0.37	1.01	up
Lysyl-Isoleucine	0.012826	-0.80	1.00	down
1-Methyl 2-galloylgalactarate	0.013386	-1.50	1.02	down
Saringosterol 3-glucoside	0.013488	-0.84	1.03	down
LysoPC(18:2(9Z,12Z))	0.013822	-0.86	1.00	down
Leu Val	0.014260	-2.20	1.01	down

8E,10E-Tetradecadienal	0.014321	-0.67	1.06	down
2-Nonadecanone	0.014348	1.28	1.00	up
Alloxanthin	0.016415	-0.71	1.05	down
N-gamma-Glutamyl-S-(1-propenyl)cysteine	0.016444	-0.99	1.05	down
Leu Thr	0.016943	-1.79	1.00	down
2,6-decadienal	0.017119	-0.57	1.03	down
Lys Lys Val Lys	0.017478	-0.81	1.04	down
TG(14:1(9Z)/18:2(9Z,12Z)/20:1(11Z))[iso6]	0.018553	-1.38	1.02	down
NH-DVal(NMe)-Val-OMe	0.019601	-2.12	1.03	down
3-trans-p-Coumaroylrotundic acid	0.019645	-1.58	1.08	down
Phe Ile	0.020094	-1.95	1.01	down
(6E,8E)-4,6,8-Megastigmatriene	0.020103	-0.56	1.02	down
LysoPC(18:4(6Z,9Z,12Z,15Z))	0.020958	-1.28	1.02	down
2-({2-[Dimethyl(2-phosphanylethyl)ammonio]ethyl} dimethylammonio)ethyl phosphinite	0.021608	-1.86	1.02	down
DG(18:2n6/0:0/20:5n3)	0.021775	-1.08	1.05	down
Ser Ile Asp Tyr	0.022722	-1.58	1.01	down
Pro Ile Asp Val	0.026973	-2.29	1.02	down
Ustiloxin A	0.029632	-2.41	1.01	down

FC = fold change. VIP = variable importance in the projection. Regulation means regulation of the amount of certain metabolite of **Ru3**-L group relative to D group.

References

[1] Najafpour MM. *Mol Cryst Liq Cryst*, 2010, 517: 167-179.

[2] Szlapa-Kula A, Malecka M, Machura B. *Dyes Pigments*, 2020, 180: 108480.

[3] Delgado J, Zhang Y, Xu B, Epstein IR. *J Phys Chem A*, 2011, 115: 2208-2215.

[4] Koizumi T, Tanaka K. *Inorg Chim Acta*, 2005, 358: 1999-2004.

[5] Santin LRR, dos Santos SC, Novo DL, Bianchini D, Gerola AP, Braga G, Caetano W, Moreira LM, Bastos EL, Romani AP, de Oliveira HPM. *Dyes Pigments*, 2015**,** 119: 12-21.

[6] Frisch MJ, Trucks GW, Schlegel HB, Scuseria GE, Robb MA, Cheeseman JR, Scalmani G, Barone V, Petersson GA, Nakatsuji H, Li X, Caricato M, Marenich AV, Bloino J, Janesko BG, Gomperts R, Mennucci B, Hratchian HP, Ortiz JV, Izmaylov AF, Sonnenberg JL, Williams-Young D, Ding F, Lipparini F, Egidi F, Goings J, Peng B, Petrone A, Henderson T, Ranasinghe D, Zakrzewski VG, Gao J, Rega N, Zheng G, Liang W, Hada M, Ehara M, Toyota K, Fukuda R, Hasegawa J, Ishida M, Nakajima T, Honda Y, Kitao O, Nakai H, Vreven T, Throssell K, Montgomery Jr. JA, Peralta JE, Ogliaro F, Bearpark MJ, Heyd JJ, Brothers EN, Kudin KN, Staroverov VN, Keith TA, Kobayashi R, Normand J, Raghavachari K, Rendell AP, Burant JC, Iyengar SS, Tomasi J, Cossi M, Millam JM, Klene M, Adamo C, Cammi R, Ochterski JW, Martin RL, Morokuma K, Farkas O, Foresman JB, Fox DJ. *Gaussian16 Revision C.01*, 2016.

[7] Andrae D, Haussermann U, Dolg M, Stoll H, Preuss H. *Theor Chim Acta*, 1990, 77 :123-141.

[8] Stephens PJ, Devlin FJ, Chabalowski CF, Frisch MJ. *J Phys Chem*, 1994, *98*: 11623-11627.

[9] Lu T, Chen FW. *J Comput Chem*, 2012, 33580-592.

[10] Humphrey W, Dalke A, Schulten K. *J Molec Graphics*, 1996, 14: 33-38.

[11] Redmond RW, Gamlin JN. *Photochem Photobiol*, 1999, 70: 391-475.

[12] Jinn SW, Beisl D, Mitchell T, Chen JN, Stainier DYR. *Development*, 2005, 132: 5199-5209.

[13] Ryan RT, Stevens KC, Calabro R, Parkin S, Mahmoud J, Kim DY, Heidary DK, Glazer EC, Selegue JP. *Inorg Chem*, 2020, 59: 8882-8892.

[14] Paul S, Kundu P, Kondaiah P, Chakravarty AR. *Inorg Chem*, 2021, 60: 16178-16193.

[15] He GL, Xu N, Ge HY, Lu Y, Wang R, Wang HX, Du JJ, Fan JL, Sun W, Peng XJ. *ACS Appl Mater Interfaces*, 2021, 13: 19572-19580.

[16] Lameijer LN, Ernst D, Hopkins SL, Meijer MS, Askes SHC, Le Dévédec SE, Bonnet S. *Chem-Eur J*, 2016, 22: 18484-18491.

[17] Liu BQ, Gao YB, Jabed MA, Kilina S, Liu GQ, Sun WF. *ACS Appl Bio Mater*, 2020, 3: 6025-6038.

[18] Lameijer LN, Breve TG, van Rixel VHS, Askes SHC, Siegler MA, Bonnet S. *Chem-Eur J*, 2018, 24: 2709-2717.